Avian reovirus-triggered apoptosis enhances both virus spread and the processing of the viral nonstructural muNS protein

Javier Rodríguez-Grille, Lisa K.Busch, José Martínez-Costas, Javier Benavente

Accepted Manuscript

AVIAN REOVIRUS-TRIGGERED APOPTOSIS ENHANCES BOTH VIRUS SPREAD AND THE PROCESSING OF THE VIRAL NONSTRUCTURAL muNS PROTEIN

AUTHORS:
Javier Rodríguez-Grille, Lisa K. Busch, José Martínez-Costas, Javier Benavente*

AFFILIATION:
Centro de Investigación en Química Biológica y Materiales Moleculares, Universidad de Santiago de Compostela, Santiago de Compostela, Spain

RUNNING TITLE:
Characterization of avian reovirus muNS processing

Key words: avian reovirus; muNS; apoptosis; caspase; proteolytic processing; viroplasms; virus spread.

Abstract: 144 words

*** Correspondence to: Centro de Investigación en Química Biológica y Materiales Moleculares, Despacho D3.7. Universidad de Santiago de Compostela, 15782-Santiago de Compostela, Spain. Tel.: 34-881815734; fax: 34-881815768; E-mail address: franciscojavier.benavente@usc.es (J. Benavente).**

Abstract

Avian reovirus non-structural protein muNS is partially cleaved in infected chicken embryo fibroblast cells to produce a 55-kDa carboxyterminal protein, termed muNSC, and a 17-kDa aminoterminal polypeptide, designated muNSN. In this study we demonstrate that muNS processing is catalyzed by a caspase 3-like protease activated during the course of avian reovirus infection. The cleavage site was mapped by site directed mutagenesis between residues Asp-154 and Ala-155 of the muNS sequence. Although muNS and muNSC, but not muNSN, are able to form inclusions when expressed individually in transfected cells, only muNS is able to recruit specific ARV proteins to these structures. Furthermore, muNSC associates with ARV factories more weakly than muNS, sigmaNS and lambdaA. Finally, the inhibition of caspase activity in ARV-infected cells does not diminish ARV gene expression and replication, but drastically reduces muNS processing and the release and dissemination of progeny viral particles.

Introduction

Avian reoviruses (ARVs) are important pathogens that cause great economic losses in the poultry industry. Infection by these viruses has been associated with a variety of disease conditions, including viral arthritis, chronic respiratory diseases, and malabsorption syndrome (Jones, 2000; van der Heide, 2000). ARVs are members of the *Orthoreovirus* genus, one of the 12 genera of the *Reoviridae* family. They are non-enveloped fusogenic viruses whose particles contain 10 double-stranded RNA genome segments enclosed within two concentric protein shells (Benavente and Martínez-Costas, 2007). Viral genomic segments can be separated electrophoretically into three different size classes, named L (Large; three segments), M (Medium; three segments) and S (Small; four segments). The ARV genome expresses at least 8 structural and four non-structural proteins (Bodelón et al., 2001), but the protein repertoire of ARV is increased to at least 12 structural proteins and six non-structural proteins by post-translational cleavage of some viral proteins (Busch et al., 2011; Ji et al., 2010; Varela et al., 1996).

Genome replication and assembly of ARVs takes place in distinctive cytoplasmic globular inclusions called viral factories where viral components concentrate to increase the efficiency of these processes (Benavente and Martinez-Costas; 2006; Tourís-Otero et al., 2004a). The framework of the factories is thought to be formed by the non-structural muNS protein, because it is the only viral protein that accumulates in factory-like inclusions when expressed individually in transfected cells (Touris-Otero et al., 2004b). Furthermore, the fact that viral core protein lambdaA and the non-structural protein sigmaNS redistribute to inclusions when individually co-expressed with muNS

in transfected cells, suggests that muNS is able to recruit these proteins to viral factories of infected cells (Tourís-Otero et al., 2004a).

Similar to many other viruses, ARVs induce apoptotic cell death of infected cells, and the activation of the intracellular apoptotic program takes place during an early stage of the ARV life cycle (Labrada et al., 2002). Apoptosis is triggered by ARV in the absence of viral gene expression, but is no longer induced when intracellular viral uncoating is blocked, suggesting both that apoptosis does not depend on viral protein synthesis and that it is triggered from within the infected cell by viral products generated after intraendosomal uncoating of parental reovirions (Labrada et al., 2002). A previous report revealed that the M3 gene of ARV expresses three muNS isoforms in infected cells and that the two smaller isoforms originate by a specific post-translational cleavage near the amino terminus of muNS. This cleavage produces a 55-kDa carboxyterminal protein, termed muNSC, and a complementary 17-kDa aminoterminal polypeptide, designated muNSN. Cleavage of muNS occurs with ~30% efficiency, so precursor muNS and its cleavage products are all present in ARV-infected cells (Busch et al., 2011). In this study we show that muNS processing is indirectly promoted by ARV infection through activation of an effector caspase that cleaves muNS between amino acid residues 154 and 155.

Results

Cleavage of ARV muNS is promoted by ARV infection

We have previously shown that ARV muNS is cleaved in ARV-infected cells to produce the aminoterminal peptide muNSN and the carboxyterminal protein muNSC (Busch, et al., 2011). To assess whether muNS cleavage is promoted by avian reovirus proteins and/or by changes induced in the host during infection, we compared muNS-to-muNSC conversion in ARV-infected cells with that in transfected cells and in insect cells infected with a muNS-expressing recombinant baculovirus (Fig. 1A). For this, extracts from CEF monolayers either mock-infected (lane 1) or infected with ARV S1133 (lane 2), from CEF monolayers transfected with either empty pCINeo plasmid (lane 3) or pCINeo-muNS plasmid (lane 4), and from Sf9 cells infected with either wild-type baculovirus (lane 5) or recombinant baculovirus AcNPV-S1133-muNS (lane 6), were subjected to immunoprecipitation (upper panel) and immunoblot (lower panel) analysis. The results revealed that while a significant amount of muNSC was generated in ARV-infected cells (its position is marked with an asterisk at the left of lane 2), this protein was hardly detected in transfected cells (lane 4) or in insect cells infected with a muNS-expressing recombinant baculovirus (lane 6). These data strongly suggest that intracellular processing of muNS is promoted by ARV infection.

Two additional experiments were subsequently performed to confirm this suggestion. In the first one, a plasmid expressing GFP fused to the amino terminus of muNS (GFP-muNS) was lipofected into CEF monolayers and 10 h later the monolayers were mock-infected or infected with ARV S1133 for 16 h. Extracts from these cells were analyzed by Western blotting using antibodies specific for both muNS and GFP. The results shown in Fig. 1B revealed that while cleavage products derived from GFP-muNS were

not detected in mock-infected cells (lanes 1 and 3), a ~45-kDa polypeptide that was recognized by antibodies against both GFP and muNS was present in ARV-infected cells (lanes 2 and 4). Its electrophoretic mobility and its capacity to interact with the two antibodies suggest that this polypeptide is GFP-muNSN. In the second confirmation experiment (Fig. 1C), ^{35}S-labeled in-vitro-generated muNS (lane 2) was incubated with extracts obtained from either mock-infected cells (lane 3) or ARV-infected cells (lane 4), and the resulting samples, as well as radiolabeled extracts from ARV-infected CEF that had been immunoprecipitated against muNS (lane 1), were analyzed by SDS-PAGE and autoradiography. The results revealed that muNS-to-muNSC conversion took place in the sample incubated with extracts from ARV-infected cells (lane 4), but not in the one incubated with extracts from mock-infected cells (lane 3). Taken together, these results indicate that muNS cleavage is promoted by ARV infection.

ARV-triggered apoptosis causes muNS processing

The muNS protein expressed by three different ARV isolates is processed to a similar extent in infected CEF cells (Fig. 1D, lanes 2-4), indicating that muNS processing is not a unique property of the ARV S1133 isolate, but a more general property of ARVs. To assess whether muNS cleavage is influenced by cell-type specific factors we examined muNS-to-muNSC conversion in cells other than CEF. The results revealed that partial cleavage of ARV muNS also takes place in ARV-infected monkey Vero cells (Fig. 1D, lane 5) and in human HeLa cells (Fig. 5A, lane 2). Surprisingly, the load of muNSC was highly reduced following infection with ARV S1133 of the CEF-

derived avian cell line DF-1 (Fig. 1D, lane 6), suggesting that muNS processing is controlled by cell factors.

The immortal DF-1 cell line was established spontaneously from Line 0 endogenous-virus negative embryos and has been widely used for the propagation of various avian viruses (Bacon et al., 2000). A genome-wide transcription profile of DF-1 cells and a comparison of their global gene expression with that of primary CEF revealed that DF-1 cells are characterized by enhanced molecular mechanisms for cell cycle progression and proliferation, suppressing cell death pathways, downregulation of caspase 3, altered cellular morphogenesis, and accelerated capacity for molecule transport (Kong et al., 2011). The observation that reduced caspase activity of DF1 cells is accompanied by diminished muNS processing when ARV infects these cells raise the interesting possibility that caspase activation and muNS cleavage are interlinked events. This hypothesis is reinforced by our finding that muNS is not processed when expressed in baculovirus-infected cells (Fig. 1A), probably because baculoviruses express anti-apoptotic factors that prevent caspase activation (Clem, 2007; Clem et al., 1991), although this awaits experimental confirmation. To explore whether there was a connection between caspase activity and muNS processing we first investigated the effect that two broad-spectrum caspase inhibitors, Z-VAD-FMK and Q-VD-OPh, exert on these processes when added to ARV-infected cells at the onset of the infection. The effect of these inhibitors on the apoptotic state of infected cells was monitored by two different approaches. In the first one, we used immunofluorescence analysis of histone H2AX phosphorylation to determine the percentage of cells containing damaged DNA (Cook et al., 2009; Yuan et al., 2010). For this, the cells were fixed, stained with a monoclonal antibody against phosphorylated H2AX and counterstained with DAPI. Polyclonal antiserum against the nonstructural muNS protein was also used to visualize

ARV-infected cells (Fig. 2A). Quantification of the stained cells revealed that, similar to staurosporine treatment (lane 5), ARV infection caused a 10 fold increase in the percentage of cells containing phosphorylated H2AX (compare lanes 1 and 4). However, this increase was highly attenuated when the infected cells were incubated in the presence of either of the two caspase inhibitors (lanes 2 and 3). In the second approach, we used the luminiscent Caspase-Glo 3/7 Assay kit (Promega) for measuring caspase-3/7 activities. The cells were lysed in Caspase-Glo 3/7 substrate and protease activity was measured as relative light units (RLU). The results shown at the bottom of Fig. 2B indicated that infection of CEF cells with ARV induced a 10 fold increase in caspase activity, but this increase was significantly reduced when the infected cells were incubated in the presence of either of the two pancaspase inhibitors.

Once demonstrated that the two inhibitors were highly efficient in preventing ARV-induced caspase activation, we next examined their capacity to prevent muNS processing in ARV-infected cells. Both immunoblotting and immunoprecipitation analysis of extracts from ARV-infected CEF revealed that muNS-to-muNSC conversion was dramatically reduced when the cells were incubated in the presence of either of the two inhibitors (Fig. 2C, compare lane 1 with lanes 2 and 3). In subsequent experiments we exclusively used the inhibitor Q-VD-OPh because it blocks apoptosis at very low nontoxic concentrations, and also because it inhibits caspase activity, but not cathepsin activity (Caserta et al., 2003; Kuželová et al., 2011). The results shown in Fig. 2D revealed that the ability of Q-VD-OPh to inhibit both apoptosis and muNS processing in ARV-infected CEF was dose-dependent, and further showed that the load of muNSC was drastically reduced at a Q-VD-OPh concentration as low as 5 μM. A time course of muNS processing and caspase activation performed in ARV-infected cells in the presence or absence of Q-VD-OPh (Fig. 2E) revealed that even though the presence of

muNS was first detected at 3 hpi, muNSC was not detected until 6 hpi, coinciding with a large increase in caspase 3/7 activity. Furthermore, both muNS processing and an increase in caspase activity were not observed when Q-VD-OPh was present during the infection (Fig. 2E, +Q). Taken together, these results strongly suggest that there is a correlation between ARV-induced apoptosis and muNS processing.

To confirm this suggestion additional experiments were performed. We first observed that the capacity of extracts of ARV-infected cells to cleave in-vitro-synthesized muNS was largely abolished when the infected cells were incubated in the presence of Q-VD-OPh (Fig. 3A, compare lanes 1 and 2). Additionally, the reduced ability of ARV to induce muNS processing in DF-1 cells was significantly enhanced when the cells were incubated during the last 6 h of infection with the pro-apoptotic agents actinomycin D and staurosporine (Fig. 3B, compare lane 1 with lanes 2 and 4), but the ability of these compounds to enhance muNS processing was blocked in the presence of the apoptotic inhibitor Q-VD-OPh (Fig. 3B, lanes 3 and 5). Finally, these pro-apoptotic agents were also effective in promoting muNS processing in transfected cells (Fig. 3C). Our findings that caspase inhibitors prevent muNS processing in ARV-infected cells and that apoptosis enhancers promote muNS cleavage in both transfected cells and ARV-infected DF1 cells indicate that muNS cleavage is catalyzed by an effector caspase activated during ARV infection.

Mapping the muNS cleavage site

In a first attempt to map the muNS cleavage site we compared the electrophoretic mobility of muNSC with that of several muNS amino-terminal truncations whose

translation initiates at different internal methionine codons (Fig. 4A). Plasmids expressing these truncations (lanes 3-5) and full-length muNS (lane 2) were transfected into CEF and the transfected cells, as well as ARV-infected CEF (lane 1), were incubated with [^{35}S]amino acids at 24 h after transfection or 16 hpi. The cells were lysed with RIPA buffer, the extracts immunoprecipitated with muNS-specific antiserum and the resulting samples analyzed by SDS-PAGE and autoradiography. The results revealed that muNSC migrates slightly faster than the muNS truncation 140-635, suggesting that the cleavage site should be located several residues downstream of Met-140 (Fig. 4A). A similar conclusion has been recently reached when comparing the electrophoretic mobility of muNSC with that of in-vitro-translated muNS truncations (Busch et al., 2011). A survey of the deduced amino acid sequence downstream of Met-140 for an appropriate caspase cleavage motif revealed the presence of the sequence ^{151}DSPD↓A^{155} (Fig. 4B, underlined), which is a canonical cleavage motif for caspases 3 and 7 (DXXD↓Y; "X" indicates any amino acid; "Y" indicates G, A, T, S or N) (Thornberry et al., 1997; Timmer and Salvesen, 2007). To verify that this putative caspase recognition sequence is a bona fide cleavage site we first examined whether the electrophoretic mobility of muNS, muNSC and muNSN matched that of transiently expressed polypeptides comprising muNS residues 1-635, 155-365 and 1-154, respectively (Fig. 4C). ARV-infected CEF (lanes 1 and 6), as well as cells lipofected with empty plasmid (lane 2) or with plasmids expressing the muNS sequences depicted on top of Fig. 4C (lanes 3-5), were radiolabeled with [^{35}S]amino acids and lysed in RIPA buffer. The resulting extracts were immunoprecipitated with polyclonal anti-muNS serum and the imunoprecipitated proteins resolved on an electrophoresis gel system (8% tricine–SDS-PAGE gel) specifically designed to resolve small peptides (Schägger, 2006). The results revealed that the muNS, muNSC and muNSN proteins

present in ARV-infected cells (Fig. 4C, lane 1) have the same electrophoretic mobility as the muNS-derived recombinant polypeptides comprising residues 1-635, 155-635 and 1-154, respectively (Fig. 4C, lanes 3-5). It should be however noted that partial conversion of muNS to muNSC took place in transfected CEF cells when the cell monolayers were kept in serum-free medium for more than 5 h during lipofection (Fig. 4C, lane 3). This is probably due to the fact that apoptosis is induced when the cells are incubated for long periods of time in serum-free medium (not shown).

To confirm that muNS is cleaved after Asp-154 we next mutated this residue to Ala and investigated abrogation of cleavage. To rule out the possibility that a function of the protein other than proteolysis could be modified by the mutation, we examined the capacity of the D154A mutant to form inclusions and to recruit the viral proteins lambdaA and sigmaNS to these structures. The immunofluorescent images shown in Fig. 4D revealed that the single site mutant D154A maintained the ability of wild-type muNS to form inclusions (lane 1) and to recruit the two ARV proteins to these structures (compare top and bottom rows of lanes 2 and 3). These observations suggest that the D-to-A mutation does not significantly alter the spatial conformation and activity of the nonstructural viral protein. We next compared the capacity of staurosporine to promote processing of both wild-type muNS and its D154A mutant in transfected cells. The results revealed that staurosporine promoted the cleavage of wild-type muNS, but not of the mutant D154A, in transfected cells (Fig. 4E). Similarly, extracts of ARV-infected CEF promoted the cleavage of wild-type muNS, but not of the D154A mutant (Fig. 4F). Taken together, these observations indicate that ARV muNS is cleaved by caspases between muNS residues Asp-154 and Ala-155.

muNS cleavage is catalyzed by a caspase 3-like protease

The results presented so far indicated both that muNS cleavage is catalyzed by a caspase and that caspase 3 and/or caspase 7 are activated in ARV infected cells. Our observation that muNS cleavage takes place in ARV-infected cells of both avian and mammalian origin indicates that muNS is a substrate for avian and mammalian caspases. To assess the role of caspase 3 in muNS processing we compared muNS-to muNSC conversion in ARV-infected HeLa and MCF-7 human cells. HeLa is a caspase 3-competent cell line, whereas MCF-7 is a breast cancer cell line that does not express a functional caspase 3 due to a 125 bp deletion in exon 3 of the caspase 3 gene (Jänicke, 2009). The results of the immunoblot analysis shown in Fig. 5A revealed that muNS-to-muNSC conversion took place in ARV-infected HeLa cells (lane 2) and that this conversion was prevented by the pancaspase inhibitor Q-VD-OPh (lane 3). However, muNS-to-muNSC conversion did not occur in ARV-infected MCF-7 cells (lane 5), even when these cells were treated for the last 6 h of infection with pro-apoptotic staurosporine (lane 6). This result suggests that caspase 3 or a protease activated by caspase 3 is directly involved in the cleavage of muNS.

We next examined whether a recombinant muNS protein purified from baculovirus-infected insect cells is a substrate for active caspases 3 and 7 of human origin available commercially. The samples obtained when muNS was incubated with these caspases, either in the presence or absence of Q-VD-OPh, as well as an extract of ARV-infected CEF, were subjected to Western blot analysis with muNS-specific antiserum. The results shown in Fig. 5B revealed that partial muNS-to-muNSC conversion occurred in the samples incubated with caspase 3, and that this conversion was prevented by the pancaspase inhibitor Q-VD-OPh. Although the result shown in lane 5 of Fig. 5B

appears to suggest that muNS is not a substrate for caspase 7, a faint band with the same electrophoretic mobility as muNSC, which disappears in the presence of Q-VD-OPh, was detected in some caspase 7 incubations after long exposures of the membrane (not shown).

Distinctive properties of muNS isoforms

We first analyzed the capacity of the three muNS isoforms to form inclusions and to recruit other viral proteins to these structures. The pictures shown in Fig. 6A revealed that both muNS and muNSC, but not muNSN, collected into globular inclusions when individually expressed in transfected cells. Furthermore, all muNS truncations containing the intercoil region (residues 477-542) including muNSC, but not HA-tagged muNSN, collected into inclusions when co-expressed with muNS (Brandariz-Nuñez et al., 2010a). However, these results should be taken with caution, since the attached tag could modify the properties of the proteins. On the other hand, the immunofluorescent images presented in Fig. 6B showed that muNS, but not muNSC, was able to recruit lambdaA and sigmaNS to inclusions (compare lanes 2 and 3). This result suggests that the portion of muNS corresponding to muNSN contains sequences required for the interaction with each of the two ARV proteins.

We next examined the strength with which muNS and muNSC associate with ARV factories. For this we compared the capacity of a Triton-X-100-containing buffer (TX) to extract muNS and muNSC from ARV-infected cells. This buffer has been previously used to discriminate between soluble and cytoskeleton-associated mammalian reovirus proteins, as well as soluble and inclusion-associated ARV proteins (Mora et al., 1987;

Tourís-Otero et al., 2004a). In the first approach, mock-infected (Fig. 6C, lanes 1 and 3) and ARV-infected CEF (Fig. 6C, lanes 2 and 4) were lysed with the Triton-X-100-containing buffer and the extracts resolved into TX-soluble (lanes 1 and 2) and TX-insoluble (lanes 3 and 4) fractions. The resulting samples were subjected to Western blot analysis with muNS-specific antiserum. The results revealed that while similar amounts of muNS are present in the TX-soluble and -insoluble fractions, most muNSC was extracted by the TX buffer. In the second approach, ARV-infected cells were pulsed with [^{35}S]amino acids for 10 min, then chased in nonradioactive medium for different time periods, and finally fractionated into TX-soluble and -insoluble fractions. The samples were immunoprecipitated with muNS-specific antiserum and analyzed by 8% tricine–SDS-PAGE and autoradiography (Fig. 6D). The results revealed that newly-synthesized muNS and sigmaNS distributed between the two fractions, with a slightly higher proportion in the TX-insoluble fraction. In contrast, most muNSC and almost all muNSN were extracted by the TX buffer at all chasing times. The reliability of the extracting procedure was evidenced by the finding that the structural protein lambdaA coimmunoprecipitated with muNS exclusively in the TX-insoluble fraction at all chasing times (lanes 6-8). These findings indicate that muNS, sigmaNS and lambdaA associate with ARV factories more tightly than muNSC, despite that muNSC, but not lambdaA or sigmaNS, collects into inclusions when individually expressed in transfected cells.

Effect of caspase inhibition on ARV replication and spread

It was of interest to determine the role that muNS processing plays on ARV replication. In the absence of an established reverse genetics system for ARV that would allow us to generate a recombinant virus that expresses an uncleavable muNS protein, like D154A, we examined the effect of Q-VD-OPh on ARV replication in CEF cells, since this compound has been shown to block both apoptosis and muNS processing. The Western blot shown in Fig 7A revealed that although the presence of the inhibitor from the onset of the infection completely blocks muNS processing, it does not significantly alter the intracellular concentration of the ARV nonstructural protein sigmaNS. This result indicates that apoptosis and muNS processing do not have significant effects on ARV gene expression and on stages of the virus life cycle prior to gene expression. Furthermore, the inhibitor did not significantly change the production of infective ARV particles, as determined by a virus plaque assay (Fig. 7B, total virus), indicating that both apoptosis and muNS processing are not required for the production of infective progeny in cultured cells.

We next investigated the effect of Q-VD-OPh on ARV release by titrating the infectious viral particles released into the incubation medium. The results showed that virus release was drastically reduced when the infected cells were incubated in the presence of Q-VD-OPh (Fig. 7B, released virus), suggesting that ARV-induced apoptosis enhances dissemination of progeny reovirions from infected cells. This suggestion was further supported by our finding that the presence of Q-VD-OPh during plaque assay of an ARV stock, where the agar overlay limits virus dissemination to neighboring cells, caused a significant reduction in the size of the viral plaques (Fig. 7C), suggesting that the inhibitor reduces cell-to-cell viral spread over the different rounds of replication, release and re-infection that occur during plaque formation.

FIGURE LEGENDS:

Fig. 1. Proteolytic processing of muNS occurs in ARV-infected cells, but not in transfected or baculovirus-infected cells (A) CEF monolayers were either mock-infected (lane 1) or infected with 10 PFU/cell of ARV S1133 (lane 2) for 16 h. The same cells were transfected with either an empty pCINeo3.1 plasmid (lane 3) or with pCINeo-muNS plasmid (lane 4) for 24 h. Sf9 insect cells were infected with either wild-type baculovirus (lane 5) or with recombinant baculovirus AcNPV-S1133-muNS (lane 6) for two days. The cells in the upper panel were incubated for 1 h with 100 μCi/ml of [^{35}S]amino acids, then lysed with RIPA buffer and immunoprecipitated with muNS-specific antiserum. An immunoblot analysis of nonradiolabeled samples is shown in the lower panel. **(B)** CEF monolayers were transfected with GFP-muNS for 10 h and then mock-infected (lanes 1 and 3) or infected with 10 PFU/cell of ARV S1133 for 16 h (lanes 2 and 4). The cells were then lysed in RIPA buffer and analyzed by Western blot with polyclonal antibodies against both GFP (lanes 1 and 2) and muNS (lanes 3 and 4). **(C)** ^{35}S-radiolabeled in-vitro-synthesized muNS (lane 2) was incubated for 2 h at 37ºC with extracts from mock-infected cells (lane 3) or from ARV-infected cells (lane 4). These samples, as well as an immunoprecipitated extract of ARV-infected CEF (lane 1), were analyzed by 10% SDS-PAGE and autoradiography. Positions of protein markers are indicated on the left, and those of nonstructural ARV proteins on the right. The position of the muNSC band is marked with an asterisk. **(D)** Western blot analysis of extracts from CEF monolayers either mock-infected (lane 1) or infected for 16 h with 10 PFU/cell of the ARV isolates 1733 (lane 2), 2408 (lane 3), and S1133 (lane 4). In lane 5 the analysis was performed with an extract of Vero cells infected for 24 h with 50 PFU of ARV S1133, and in lane 6 with an extract of DF-1 cells infected for 16 h with 10

PFU of ARV S1133. The membranes in lanes 1-4 and 6 were exposed for 5 seconds and the one in lane 5 for 30 seconds.

Fig. 2. Effect of apoptosis inhibitors on muNS processing. (A) Effect of apoptotic inhibitors on DNA damage. CEF monolayers were infected with 10 PFU/cell of ARV in the absence (lane 1) or presence of either 100 μM Z-VAD-FMK (Z; lane 2) or 10 μM Q-VD-OPh (Q; lane 3). Mock-infected cells either untreated (lane 4) or incubated for 6 h in the presence of 0.5 μM staurosporine (lane 5) were used as control samples. The cells were analyzed by indirect immunofluorescence with rabbit polyclonal antibodies against muNS (upper row; green), with a monoclonal antibody against phosphorylated H2AX (middle row; red), and nuclei were stained with DAPI (lower row; blue). The percentage of red-stained nuclei shown at the bottom of the figure is the mean of three independent experiments, and 100 cells were counted for each experiment. **(B)** Effect of the same concentrations of the two apoptotic inhibitors on caspase 3/7 activity. Caspase activity was determined with the Caspase-Glo® 3/7 Assay kit (Promega), as described in the Material and Methods section, and expressed as arbitrary RLU units. Each value is the mean of three independent experiments. **(C)** Effect of the two apoptotic inhibitors on muNS processing in ARV-infected CEF. Processing was monitored by both immunoprecipitation (IP; upper panel) and Western blotting (WB; lower panel) using muNS-specific antiserum. The sample in lane 1 was run in the same gel, but an internal lane was removed. **(D)** Effect of Q-VD-OPh on muNS processing and caspase 3/7 activity. ARV-infected CEF monolayers were incubated from the onset of the infection with the concentrations of the pancaspase inhibitor shown on top. At 16 hpi the cells were lysed and the resulting extracts were assayed for caspase 3/7 activity and muNS processing. Processing of muNS was monitored by Western blotting with polyclonal

antibodies against muNS and actin. The values of caspase activity shown at the bottom of the figure are the mean of three independent experiments. **(E)** Time course of muNS processing and caspase 3/7 activity in ARV-infected CEF cells. CEF cell monolayers were infected with 10 PFU/cell of ARV, either in the absence (top blot) or presence (bottom blot) of 10 μM Q-VD-OPh. The cells were lysed at the infection times indicated at the top of the figure. The extracts were subsequently processed for both immunoblotting and caspase 3/7 activity, as for Fig. 2D.

Fig. 3. Effect of apoptosis inhibitors/enhancers on muNS processing. (A) Effect of Q-VD-OPh on muNS processing. ^{35}S-radiolabeled in-vitro-synthesized muNS was incubated for 4 h at 37ºC with extracts from ARV-infected cells that had been incubated (lane 2) or not (lane 1) with 10 μM Q-VD-OPh from the onset of the infection. These samples, as well as an extract of ARV-infected CEF immunoprecipitated against muNS (lane 3), were analyzed by 10% SDS-PAGE and autoradiography. **(B)** Effect of apoptotic enhancers and inhibitors on muNS processing and apoptosis in DF1 cells. DF-1 cell monolayers were infected with 10 PFU/cell of ARV S1133. The cells in lanes 3 and 5 were treated from the onset of the infection with 10 μM Q-VD-OPh. The cells in lanes 2 and 3 were treated from 10 to 16 hpi with 1 μg/ml actinomycin D, and in lanes 4 and 5 with 0.5 μM staurosporine. Caspase 3/7 activity, DNA damage and muNS processing were determined at 16 hpi as for Figs. 2A-C. **(C)** Effect of apoptotic enhancers and inhibitors on muNS processing in transfected cells. CEF monolayers were transfected with the pCINeo-muNS plasmid and 24 h later the cells were incubated for 6 h with the same compounds as for Fig. 3B. The cells were then lysed and the resulting extracts subjected to Western blot analysis with anti-muNS serum. The

positions of nonstructural viral proteins are indicated on the left and that of protein markers on the right.

Fig. 4. Mapping the muNS cleavage site. (A) CEF monolayers were infected with ARV S1133 (lane 1) or lipofected with plasmids expressing muNS versions comprising the residues shown on top of lanes 2-5. The cells were incubated with [^{35}S]amino acids for 1 h at 16 hpi or for 2 h at 24 h after transfection, then lysed with RIPA buffer. The resulting extracts were immunoprecipitated with muNS-specific antiserum and the samples analyzed by 8% SDS-PAGE and autoradiography. The position of a non-specific protein band in transfected cells is marked with an arrow. **(B)** Deduced amino acid sequence of the ARV S1133 muNS region comprising residues 140-177. A potential consensus cleavage sequence for caspase 3/7 is underlined and the putative cleavage site marked with an arrow. **(C)** CEF monolayers were infected with ARV S1133 (lanes 1 and 6) or transfected with empty pCINeo plasmid (lane 2) and with plasmids expressing muNS versions comprising the amino acid residues shown on top of lanes 3-5. The cells were radiolabeled with [^{35}S]amino acids for 1 h at 16 hpi or for 5 h at 24 h after transfection, lysed with RIPA buffer and the extracts immunoprecipitated with muNS-specific antiserum. Immunoprecipitated proteins were resolved on an 8% tricine-SDS-PAGE gel and protein bands visualized by autoradiography. **(D)** The D154A muNS mutant (lane 1) and the ARV proteins shown on top (lanes 2 and 3) were transiently expressed in CEF cells, either individually (top row) or in combination with D154A (bottom row). At 24 h after transfection the cells were subjected to immunofluorescence analysis using, as primary antibodies, polyclonal antiserum against muNS (lane 1), ARV cores (lane 2),and sigmaNS (lane 3). **(E)** CEF monolayers were transfected with plasmids pCINeo-muNS (lanes 1-3) and pCINeo-

D154A (lanes 4-5), and at 18 h post-transfection the cells in lanes 2, 3 and 5 were incubated for 6 h in the presence of 0.5 μM staurosporine, and the cells in lane 3 were also supplemented with 10 μM Q-VD-OPh. The cells were then lysed and subjected to Western blot analysis with anti-muNS serum. **(F)** ^{35}S-radiolabeled in-vitro-synthesized muNS (lane 1) or its D154A point mutant (lane 2) were incubated for 4 h at 37ºC with extracts from ARV-infected cells. These samples, as well as an extract of ARV-infected CEF immunoprecipitated against muNS (lane 3), were analyzed by 10% SDS-PAGE and autoradiography. The positions of protein markers are indicated on the left and those of ARV nonstructural proteins on the right.

Fig. 5. Identification of the caspase that catalyzes muNS cleavage. (A) Semiconfluent monolayers of HeLa (lanes 1-3) and MCF-7 (lanes 4-6) cells were mock-infected (lanes 1 and 4) or infected with 50 PFU/cell of ARV 1733 (lanes 2, 3, 5 and 6). The cells in lane 3 were incubated with 10 μM Q-VD-OPh from the onset of the infection and the cells in lane 6 were incubated with 0.5 μM staurosporine during the last 6 h of infection. At 16 hpi the cells were lysed in RIPA buffer and the resulting cell extracts were analyzed by Western blotting with muNS-specific antiserum. **(B)** 1 μg of recombinant muNS purified from baculovirus-infected insect cells (lane 2) was incubated with 1 unit of either caspase 3 (lanes 3 and 4) or caspase 7 (lanes 5 and 6) for 4 h at 37ºC, in the presence (lanes 4 and 6) or absence (lanes 3 and 5) of 10 μM Q-VD-OPh. These samples, as well as an extract of ARV-infected CEF (lane 1), were subjected to Western blot analysis using polyclonal anti-muNS serum. The positions of protein markers are shown on the left and those of nonstructural ARV proteins on the right.

Fig. 6. Properties of muNS, muNSC and muNSN. (A) Plasmids expressing muNS versions comprising the amino acid residues shown on top were lipofected into CEF monolayers, and at 20 h post-transfection the cells were subjected to immunofluorescence analysis with muNS-specific antiserum as primary antibody (green), and counterstained with DAPI (blue). **(B)** Plasmids expressing the ARV proteins depicted on the left were transfected into CEF monolayers either individually (lane 1) or together with plasmids expressing full-length muNS (lane 2) or muNS(155-635). At 20 h post-transfection the cells were processed for immunofluorescence using as primary antibodies polyclonal antisera against ARV cores (top row) and sigmaNS (bottom row), and counterstained with DAPI (blue). **(C)** CEF monolayers were mock-infected (lanes 1 and 3) or infected with 10 PFU/cell of ARV S1133 (lanes 2 and 4) for 16 h. The cells were then lysed with TX-buffer, incubated for 10 min on ice and the TX-soluble fraction was removed (lanes 1 and 2). The plate-attached fraction was then solubilized with RIPA buffer (TX-insoluble fraction; lanes 3 and 4). The two fractions were analyzed by Western blotting with muNS-specific antiserum. **(D)** ARV-infected cells were labeled for 10 min with [^{35}S]amino acids and then incubated in non-radioactive medium for the indicated chasing times. The cells were subsequently processed as for Fig. 2C and the resulting TX-soluble and -insoluble fractions were immunoprecipitated with muNS-specific antiserum. Immunoprecipitated proteins were resolved by electrophoresis on an 8% tricine-SDS-PAGE gel and visualized by autoradiography. Positions of protein markers are indicated on the left and those of ARV proteins on the right.

Fig. 7. Effect of Q-VD-OPh on ARV replication and dissemination. (A) CEF monolayers were mock-infected (M) or infected with 10 PFU/cell of ARV S1133 (I), in

the presence (+Q) or absence of 10 μM Q-VD-OPh. The cells were processed for immunoblotting at 16 hpi and the membranes were probed with rabbit polyclonal antibodies against both muNS and sigmaNS. The positions of protein markers are indicated on the left and those of the non-structural ARV proteins on the right. **(B)** CEF monolayers were infected with 0.1 PFU/cel of ARV S1133, and the production of both total virus (intracellular + culture medium; filled bars) and released virus (cultured medium; open bars) was determined after 24 h of infection by plaque assay on CEF monolayers. **(C)** Plaque pictures obtained by titrating a stock of ARV S1133 on CEF monolayers in the absence (lane 1) or presence (lane 2) of 10 μM Q-VD-OPh. The pictures in lane 1 correspond to a 10^6 dilution and the ones in lane 2 to a 10^5 dilution of the same virus stock. Plaques of two different plaque assays are shown.

Fig. 8. Alignment of the deduced amino acid sequences of the muNS 140-177 region from different poultry reoviruses. Source of the host birds, virus strains, deduced amino acid sequences of the muNS region 140-177 and protein accession numbers are indicated. Putative consensus caspase cleavage sequences are boxed.

Discussion

Activation of programmed cell death is one of the first protective defences set up by the host cell to restrict viral amplification and spread. When triggered early in infection apoptosis may limit both the time and the cellular machinery available for virus replication. Therefore, it is not surprising that many viruses try to overcome the apoptotic threat by using a battery of different strategies and by expressing a variety of antiapoptotic products aimed to block or delay the induction of apoptosis (Galluzzi et al., 2010). However, other viruses induce apoptosis actively at late stage of infection to facilitate virus release and spread with limited induction of inflamatory and immune host responses (Teodoro and Branton, 1997). The results shown in Fig. 2 E confirmed previous findings from our laboratory that ARV infection triggers apoptosis in cultured cells at an early stage of the viral life cycle (Labrada et al., 2002), yet the results of this study demonstrate that early apoptosis triggering does not have adverse effects on either ARV gene expression or infectious progeny production. These apparently conflicting results can be reconciled considering that ARV has a short replication time (Benavente and Martínez-Costas, 2006), which would allow the virus to proceed its life cycle successfully until completion and to reach a satisfactory intracellular production of progeny viral particles before the infected cell dies or is severely damaged by the execution of apoptosis.

A growing number of viruses have been documented to take advantage of apoptosis induction and caspase activation to promote their own replication. For instance, viruses as diverse as mammalian reovirus, human astrovirus, measles virus, porcine circovirus 2, African swine fever virus, bovine herpesvirus 1, coronavirus, influenza virus and the Moscow strain of Ectromelia virus, all have been reported to usurp apoptosis for

facilitating the release of progeny viral particles from infected cells (Best, 2008; Galluzzi et al., 2010). The results of the present study suggest that ARV should be included in that list, since this virus activates rather than suppress caspases and this activation is necessary for efficient virus release and spread. On the other hand, many apoptosis-inducing viruses express proteins that are processed by caspases to generate cleavage products with novel properties, ranging from apoptosis downregulation to enhancement or attenuation of viral replication (Richard and Tulasne, 2012). Still, the functional consequences of many protein caspase cleavages remain elusive so far, yet the conservation of caspase targets in many viral proteins and the stability of their processed products suggest that caspase cleavage of viral polypeptides could constitute an evolutionary advantage that benefits virus replication. In this study we have provided compelling evidence that caspases activated during ARV-induced apoptosis catalyze the cleavage of ARV nonstructural muNS protein to produce the 17-kDa N-terminal peptide muNSN and the 55-kDa C-terminal protein muNSC. In the literature to date, there are several examples of other non-structural viral proteins that are caspase targets, like the NS1 protein of Aleutian mink disease parvovirus, the NS5A protein of hepatitis C virus, the NS1' protein of Japanese encephalitis virus, and the EIA protein of adenovirus 12 (Best et al., 2003; Grand et al., 2002; Satoh et al., 2000; Sun et al., 2012). We also observed that a substantial amount of full-length muNS remains uncleaved both in infected cells and after 6 h of incubation with recombinant caspase 3, implying that caspase-catalyzed muNS cleavage is a regulated process, as has been reported for several cellular and viral proteins (Best et al., 2003; Chaudhry et al., 2012; Cheng et al., 2010; Mashima et al., 1999; Sun et al., 2012). Incomplete processing of a precursor viral protein could be a strategy to reduce the activity of the intact protein or it could be

used to increase the protein repertoire encoded by size-limited viral genomes, thus generating cleaved viral products with novel properties/activities.

That avian and mammalian reoviruses use different mechanisms to express their muNSC isoforms (Busch et al., 2011), and that both the muNS precursor and its truncated forms coexist in avian/mammalian reovirus-infected cells suggest that there should be distinct functional roles for both the precursor and its truncated proteins. It should be noted however that avian and mammalian reovirus muNSC proteins display different properties. Thus, while mammalian reovirus muNSC still maintains its precursor's ability to associate with the major core protein lambda1 (Miller et al., 2010), this ability is not shared by its ARV counterpart (Fig. 6B), because sequences of ARV muNS required for binding to lambdaA are lacking in muNSC. It has been reported that the release of astrovirus from infected cells depends on both the processing of the capsid precursor polypeptide VP90 and the activities of executioner caspases (Banos-Lara and Mendez, 2010). Accordingly, the possibility exists that muNS processing is required for enhanced release and dissemination of ARV, although it is unlikely, since apoptosis has also been reported to promote the release of mammalian reovirus from infected cells without enhancing the production of its muNSC protein (Marcato et al., 2007). In the absence of an established reverse genetics system for avian reoviruses, the consequences of muNS cleavage on viral replication and spread remain unclear.

Despite the facts that ARV muNSC is able to form inclusions when expressed in isolation and that it collects into inclusions when co-expressed with muNS (Brandariz-Nuñez et al., 2010), muNSC associates with factories of infected cells more weakly than full-length muNS, sigmaNS or lambdaA, as evidenced by extraction with TX buffer (Figs. 6C and 6D). This observation suggests that ARV factories are complex structures formed by a diverse array of protein-protein and protein-RNA interactions and that

these entities are much more complex than muNS-derived inclusions. This is supported by our observation that the inclusions formed by expressing muNS versions in baculovirus-infected insect cells can be easily purified (Brandariz-Nuñez et al., 2010a), whereas we were unable to purify the factories formed in ARV-infected cells.

The results shown in Fig. 5 demonstrate that muNS is a substrate for mammalian caspase 3, yet the absence of both commercial recombinant caspases of avian origin and caspase 3-deficient avian cells did not allow us to identify the avian caspase that catalyzes ARV muNS cleavage in infected avian cells. Nevertheless, this cleavage is probably catalysed by an avian caspase 3-like protease, since caspase sequences and targets are highly conserved in different species (Sakamaki and Satou, 2009), and since we found both that caspase 3/7 is active in ARV-infected avian cells and that muNS-to-muNSC processing is promoted by the caspase 3 activator staurosporine (Chae et al., 2000). The presence of a caspase 3/7 consensus sequence (^{151}DSPD↓A^{155}) within the muNS cleavage region allowed us to map the muNS cleavage site between residues Asp-154 and Ala-155, by using site-directed mutagenesis. This finding suggests that this region of muNS is placed in a flexible and exposed loop accessible to caspases. Interestingly, the caspase 3/7 consensus sequence found in ARV S1133 muNS is not fully conserved among avian reoviruses isolated from chickens, since it is only present in 8 isolates, and in one quail isolate, but not in other 9 chicken isolates. Thus, in the muNS protein from 4 chicken isolates Asp-151 is replaced by His, while in the protein from another 5 isolates Asp-151 and Ser-152 are replaced by His and Glu, respectively (Fig. 8). If cleavage of these "nonconsensus" ARV muNS proteins still occurs between Asp-154 and Ala-155 would imply that accessibility is more important than the presence of specific amino acids at positions 3 and 4 of the caspase consensus sequence, which is in agreement with previous reports indicating that caspases do not have a strict

requirement for positions 2-4 of the consensus cleavage site (Timmer and Salvesen, 2007; Thornberry et al., 1997). Curiously, the muNS protein encoded by both duck and goose reoviruses does not contain a caspase 3/7 consensus sequence spanning residues 151-155, because Asp-154 is replaced by a Gly residue. However, these muNS proteins contain two putative caspase targets, one spanning residues 142-146 (^{142}GTMDA^{146}), and the other comprising residues 156-160 (^{156}SVPDV^{160}). Surprisingly, the former caspase target is also present in the muNS protein from four chicken isolates (Fig. 8). It should be of interest to check whether duck/goose reoviruses induce apoptosis, whether the muNS protein of these viruses is cleaved in infected cells and whether its cleavage takes place at one or both of these caspase consensus sequences. Nevertheless, the presence of specific residues in the muNS 140-177 region could serve to assign a poultry reovirus as an avian/quail or a goose/duck reovirus. Thus, the muNS from reoviruses of avian/quail origin has leucine in position 144, alanine or valine in 150, aspartic acid in 154, cysteine in 156 and valine in 159, whereas the muNS from reoviruses of duck/goose origin has methionine, glycine, glycine and aspartic acid in those positions.

Methods

Cells, viruses, antibodies and reagents

Primary cultures of CEFs were prepared from 9- to 10-day-old chicken embryos and grown in monolayers in medium 199 supplemented with 10% tryptose phosphate broth and 5% calf serum. Avian DF-1, human HeLa and MCF-7, and monkey Vero cell lines, all were grown in monolayers in Dulbecco's modified Eagle's medium (DMEM; Invitrogen) supplemented with 10% fetal bovine serum (FBS). MCF-7 cells were a kind gift from María Dolores Blanco (Universidad Complutense de Madrid). Sf9 cells were grown in suspension culture in serum-free Sf-900 II media at 27º C. Strains S1133, 1733 and 2408 of avian reovirus were grown in semiconfluent monolayers of primary CEFs. Conditions for growing and titrating these viruses have been described previously (Grande and Benavente, 2000). The recombinant baculovirus AcNPV-S1133-muNS was grown in Sf9 cells as previously described (Brandaríz-Nuñez et al., 2010b).

Rabbit polyclonal sera against ARV S1133 reovirions and cores, as well as ARV S1133 proteins muNS and sigmaNS were raised in our laboratory (Touris-Otero et al., 2004b). Monoclonal anti-gamma histone H2A.X (phospho S139) antibody was purchased from Abcam plc. Rabbit anti-actin polyclonal antibody was purchased from Santa Cruz Biotechnology. Peroxidase-conjugated goat anti-rabbit antibody was purchased from Sigma. Pancaspase inhibitors Z-VAD-FMK and Q-VD-OPh were from Calbiochem. Caspases 3 and 7 were from Enzo Life Science (Cat. # C-3: ALX-201-059; C-7: ALX-201-061-U025). All other reagents were purchased from Sigma.

Viral infections and protein analysis

Semiconfluent monolayers of cells were infected with 10 PFU/cell of ARVs for the times indicated for each experiment. In all experiments, except for some of Fig. 1 and those of Fig. 5A, CEF cell monolayers were infected with the ARV S1133. For metabolic radiolabeling, the cultured medium was removed and the cells were incubated for the indicated times in methionine/cysteine-free medium containing 100 μCi/ml of [^{35}S]methionine-cysteine. For immunoprecipitation and Western blot analysis the cells were lysed in RIPA buffer (50 mM Tris–HCl pH 7.5, 150 mM NaCl, 1% NP40, 0.5% DOC, 0.1% SDS, supplemented with "Complete protease inhibitor cocktail" from Roche Diagnostics), and muNS-derived proteins were detected with a muNS-specific antiserum (Touris-Otero et al., 2004b).

To isolate TX-soluble and -insoluble fractions, 2 x 10^6 cells were lysed in 200 μl of TX buffer (10 mM Pipes pH 6.8, 3 mM $MgCl_2$, 100 mM KCl, 300 mM sucrose, 1% Triton X-100, supplemented with "Complete protease inhibitor cocktail" from Roche Diagnostics) and the soluble fraction was removed. The plates were washed again with TX buffer and the insoluble fraction that remained attached to the plates was directly solubilized in 200 μl of RIPA buffer (Tourís-Otero et al., 2004a). For pulse–chase analysis, mock-infected and reovirus-infected cells were incubated for 2 h at 12 h p.i. in medium lacking methionine and cysteine, and then incubated for 10 min in the same medium supplemented with 500 μCi/ml [^{35}S]amino acids. The cells were chased for the indicated times in non-radioactive medium supplemented with an excess of nonradiolabelled methionine and cysteine. Infection of Sf9 insect cells with the recombinant baculovirus AcNPV-S1133-muNS and purification of recombinant muNS have already been described (Brandaríz-Nuñez et al., 2010b).

Plasmid construction and cell transfection

The construction of recombinant plasmids expressing full-length ARV S1133 muNS, GFP-muNS, and the aminoterminal truncations comprising muNS residues 84-635, 127-635 and 140-635 has already been described (Brandaríz-Nuñez et al., 2010b). Plasmid pCINeo-muNS was used as template to generate constructs expressing the following proteins. The D154A muNS point mutant was generated with the QuikChange site-directed mutagenesis kit (Stratagene), according to the manufacturer's specifications. The forward primer was: 5' CCACCGCTGATTCCCCCGCTGCCTGCGTCCCAGTCACC 3'; and the reverse primer was: 5' GGTGACTGGGACGCAGGCAGCGGGGGAATCAGCGGTGG 3'. To generate the construct expressing muNS(1-154), the forward primer was: 5' GCGGAATTCATCATGGCGTCAACCAAGTGG 3'; and the reverse primer was: 5' GCGTCTAGATTAATCGGGGGAATCAGCGGTGG 3'. To generate the construct expressing muNS (155-635), the forward primer was: 5' GCGGAATTCATCATGGCCTGCGTCCCAGTC 3'; and the reverse primer was: 5' GCGTCTAGATCACAGATCATCCACCAATTCTTC 3'. The correctness of the recombinant plasmids was confirmed by nucleotide sequencing.

Transfection of preconfluent cell monolayers was done using Lipofectamine Plus reagent (Invitrogen) following the manufacturer´s instructions, with 1 μg of DNA per well of a 12-well dish. Transfected cells were incubated at 37ºC for 24 h, unless otherwise stated.

Indirect immunofluorescence microscopy

Cell monolayers grown on coverslips were infected or transfected as indicated in the figure legends. At the indicated times, the monolayers were washed twice with PBS and fixed in paraformaldehyde for 15 min at 4ºC. Fixed cells were washed twice with PBS, incubated for 10 min in permeabilizing buffer (0.1% Triton X-100 in PBS), incubated 20 min with blocking buffer (2% BSA in PBS), and then incubated for 1 h at room temperature with primary antibodies diluted in blocking buffer. The cells were washed three more times with PBS and then incubated with secondary antibodies and DAPI (4,6-diamidino-2-phenylindole) for 1 h at room temperature. Coverslips were then washed six times with PBS and mounted on glass slides. Images were obtained with an Olympus DP-71 digital camera mounted on an Olympus BX51 fluorescence microscope. Images were processed with Adobe Photoshop (Adobe Systems).

In vitro transcription and translation

The recombinant plasmids used as templates were linearized with NotI, purified by extraction with phenol/chloroform, precipitated with ethanol and resuspended in sterile water at a final concentration of 1 mg/ml. In vitro transcription from the T7 promoter was performed by using a RiboMAX Large Scale RNA Production System (Promega). In vitro translation was carried out by using a Rabbit Reticulocyte Lysate System (nuclease-treated; Promega) following the manufacturer's instructions, for 90 min at 30º

C in the presence of 50 mg/ml RNA and 0.4 mCi/ml [^{35}S]methionine (Hartmann analytic KSM-01).

Intracellular caspase activity and in vitro protease cleavage assays

The intracellular activity of caspases 3/7 was determined with the Caspase-Glo® 3/7 Assay kit from Promega, following the manufacturer's instructions.

In vitro caspase cleavage assays were performed by mixing 1 µg of muNS purified from baculovirus-infected insect cells, as described previously (Brandariz-Nuñez et al., 2010a), with 1 unit of recombinant caspase in 10 µl of caspase buffer (20 mM Hepes pH 7.4; 100 mM NaCl; 0.05% NP-40). In some samples 10 µM of the pancaspase inhibitor Q-VD-OPh was also included. Mixtures were incubated for 4 h a 37ºC, mixed with 5 µl of 3x Laemmli electrophoresis sample buffer and boiled for 5 min at 100ºC. Cleavage of muNS was analyzed by Western blotting.

To evaluate the capacity of extracts of ARV-infected cells to promote muNS cleavage, extracts from mock-infected and infected cells were prepared as follows. Samples of 2 x10^7 CEF cells, mock-infected or infected with 0.1 PFU/ml of ARV S1133, in the presence or absence of 10 µM Q-VD-OPh, were washed twice with PBS at 24 hpi and overlayed with 1 ml of caspase buffer. The cells were then collected by scrapping and lysed by one cycle of freezing and thawing. A typical protease cleavage assay was performed by mixing 5 µl of cell extract with 5 µl of reticulocyte lysate containing ^{35}S-radiolabeled muNS or its D154A mutant. Samples were incubated for 2 h at 37ºC, then supplemented with 5 µl of 3x Laemmli sample buffer and boiled for 5 min at 100ºC. Processing of muNS was monitored by SDS-PAGE and autoradiography.

Acknowledgments

We would like to thank Rebeca Menaya for technical assistance and other members of our laboratory for helpful discussions on the manuscript. We also thank Laboratorios MSD España (Salamanca, Spain) for providing pathogen-free embryonated eggs. This work was funded by grants from the Spanish Ministerio de Economia y Competitividad (BFU2010-22228) and from the Xunta de Galicia (CN 2012/018).

References

Bacon, L.D., Hunt, H.D., Cheng, H.H., 2000. A review of the development of chicken lines to resolve genes determining resistance to diseases. Poult. Sci. 79, 1082-1093.

Banos-Lara, M.R., Mendez, E., 2010. Role of individual caspases induced by astrovirus on the processing of its structural protein and its release from the cell by a non-lytic mechanism. Virology 401, 322-332.

Benavente J., Martinez-Costas J., 2006. Early steps in avian reovirus morphogenesis. Curr. Top. Microbiol. Immunol. 309, 67–85.

Benavente, J., Martinez-Costas, J., 2007. Avian reovirus: structure and biology. Virus Res. 123, 105–119.

Best, S.M., 2008. Viral subversion of apoptotic enzymes: escape from death row. Annu. Rev. Microbiol. 62, 171-192.

Best, S.M., Shelton, J.F., Pompey, J.M., Wolfinbarger, J.B., Bloom, M.E., 2003. Caspase cleavage of the non-structural protein NS1 mediates replication of Aleutian mink disease parvovirus. J. Virol. 77, 5305-5312.

Bodelon, G., Labrada, L., Martinez-Costas, J., Benavente, J., 2001. The avian reovirus genome segment S1 is a functionally tricistronic gene that expresses one structural and two nonstructural proteins in infected cells. Virology 290, 181–191.

Brandariz-Nuñez, A., Menaya-Vargas, R., Benavente, J., Martinez-Costas, J., 2010a. A versatile molecular tagging method for targeting proteins to avian reovirus muNS inclusions. Use in protein immobilization and purification. PLoS ONE 5, e13961.

Brandariz-Nuñez, A., Menaya-Vargas, R., Benavente, J., Martinez-Costas, J., 2010b. Avian reovirus muNS protein forms homo-oligomeric inclusions in a microtubule-

independent fashion, which involves specific regions of its C terminal domain. J. Virol. 84, 4289–4301.

Busch, L.K., Rodriguez-Grille, J., Ignacio Casal, J., Martinez-Costas, J., Benavente, J., 2011. Avian and mammalian reoviruses use different molecular mechanisms to synthesize their μNS isoforms. J. Gen. Virol. 92, 2566–2574.

Caserta, T.M., Smith, A.N., Gultice, A.D., Reedy, M.A., Brown, T.L., 2003. Q-VD-OPh, a broad spectrum caspase inhibitor with potent antiapoptotic properties. Apoptosis 8, 345-352.

Chae, H-J., Kang, J-S., Byun, J-O., Han, K-S., Kim, D-U., Oh, S-E., Kim, H-M., Chae, S-W., Kim, H-R., 2000. Molecular mechanism of staurosporine-induced apoptosis in osteoblasts. Pharmacol. Res. 42, 373-381.

Chaudhry, P., Singh, M., Parent, S., Asselin, E., 2012. Prostate apoptosis response 4 (Par-4), a novel substrate of caspase 3 during apoptosis activation. Mol. Cell Biol. 32, 826-839.

Cheng, F., Chen, A.Y., Best, S.M., Bloom, M.E., Pintel, D., Qiu, J., 2010. The capsid proteins of Aleutian mink disease virus activate caspases and are specifically cleaved during infection. J. Virol. 84, 2687-2696.

Clem R.J., 2007. Baculoviruses and apoptosis: a diversity of genes and responses. Curr. Drug targets 8, 1069-1074.

Clem, R.J., Fechheimer, M., Miller, L.K., 1991. Prevention of apoptosis by a baculovirus gene during infection of insect cells. Science 254, 1388-1390.

Cook, P.J., Ju, B.G., Telese, F., Wang, X., Glass, C.K., Rosenfeld, M.G., 2009. Tyrosine dephosphorylation of H2AX modulates apoptosis and survival decisions. Nature 458, 591–596.

Galluzzi, L., Kepp, O., Morselli, E., Vitale, I., Senovilla, L., Pinti, M., Zitvogel, L., Kroemer, G., 2010. Viral strategies for the evasion of immunogenic cell death. J. Intern. Med. 267, 526–542.

Grand, R.J.A., Schmeiser, K., Gordon, E.M., Zhang, X., Gallimore, P.H., Turnell, A.S., 2002. Caspase-mediated cleavage of adenovirus early region 1A proteins. Virology 301, 255–271.

Grande, A., Benavente, J., 2000. Optimal conditions for the growth, purification and storage of the avian reovirus S1133. J. Virol. Methods 85, 43–54.

Jänicke, R.U., 2009. MCF-7 breast carcinoma cells do not express caspase-3. Breast Cancer Res. Treat. 117, 219-221.

Ji, W.T., Lin, F.L., Wang, Y.C., Shih, W.L., Lee, L.H., Liu, H.J., 2010. Intracellular cleavage of σA protein of avian reovirus. Virus Res. 149, 71–77.

Jones, R.C., 2000. Avian reovirus infections. Rev. Sci. Tech. 19, 614–625.

Kong, B.W., Lee, J.Y., Bottje, W.G., Lassiter, K., Lee, J., Foster, D.N., 2011. Genome-wide differential gene expression in immortalized DF-1 chicken embryo fibroblast cell line. BMC Genomics 12, 571.

Kuželová, K., Grebeňová, D., Brodská, B., 2011. Dose-dependenteffects of the caspase inhibitor Q-VD-OPh on different apoptosis-related processes. J. Cell Biochem. 112, 3334-3342.

Labrada, L., Bodelon, J., Viñuela, J., Benavente, J. 2002. Avian reoviruses cause apoptosis in cultured cells: viral uncoating, but not viral gene expression, is required for apoptosis induction. J. Virol. 76, 7932–7941.

Marcato, P., Shmulevitz, M., Pan, D., Stoltz, D., Lee, P.W., 2007. Ras transformation mediates reovirus oncolysis by enhancing virus uncoating, particle infectivity, and apoptosis-dependent release. Mol. Ther. 15, 1522-1530

Mashima, T., Naito, M., Tsuruo, t., 1999. Caspase-mediated cleavage of cytoskeletal actine plays a positive role in the process of morphological apoptosis. Oncogene 18, 2423-2430.

Miller, C.L., Arnold, M.M., Broering T.J., Hastings, C.E., and Nibert, M.L., 2010. Localization of mammalian orthoreovirus proteins to cytoplasmic factory-like structures via nonoverlapping regions of μNS. J. Virol. 84, 867-882.

Mora, M., Partin, K., Bhatia, M., Partin, J., Carter, C., 1987. Association of avian reovirus proteins with the structural matrix of infected cells. Virology 159, 265–277.

Richard, A., Tulasne, D., 2012. Caspase cleavage of viral proteins, another way for viruses to make the best of apoptosis. Cell Death Dis. 3, e277.

Sakamaki, K., Satou, Y., 2009. Caspases: evolutionary aspects of their functions in vertebrates. J. Fish Biol. 74, 727-753.

Satoh, S., Hirota, M., Noguchi, T., Hijikata, M., Handa, H., Shimotonot, k., 2000. Cleavage of hepatitis C virus nonstructural protein 5A by a caspase-like protease(s) in mammalian cells. Virology 270, 476-487.

Schägger, H., 2006. Tricine-SDS-PAGE. Nature Protoc. 1, 16-22

Sun, J., Yu, Y., Deubel, V., 2012. Japanese encephalitis virus NS1' protein depends on pseudoknot secondary structure and is cleaved by caspase during virus infection and cell apoptosis. Microbes Infect. 14, 930-940.

Teodoro, J.G., Branton, P.E., 1997. Regulation of apoptosis by viral gene products. J. Virol. 71, 1739-1746.

Thornberry, N.A., Rano, T.A., Peterson, E.P., Rasper, D.M., Timkey, T., Garcia Calvo, M., Houtzager, V.M., Nordstrom, P.A., Roy, S., Vaillancourt, J.P., Chapman, K.T., Nicholson, D.W., 1997. A combinatorial approach defines specificities of members

of the caspase family and granzyme B. Functional relationships established for key mediators of apoptosis. J. Biol. Chem. 272, 17907-17911.

Timmer, J.C., Salvesen, G.S., 2007. Caspase substrates. Cell Death Differ. 14, 66-72.

Touris-Otero, F., Cortez-San Martin, M., Martinez-Costas, J., Benavente, J., 2004a. Avian reovirus morphogenesis occurs within viral factories and begins with the selective recruitment of σNS and λA to μNS inclusions. J. Mol. Biol. 341, 361–374.

Touris-Otero, F., Martinez-Costas, J., Vakharia, V.N., Benavente, J., 2004b. Avian reovirus nonstructural protein μNS forms viroplasm-like inclusions and recruits protein σNS to these structures. Virology 319, 94–106.

van der Heide, L., 2000. The history of avian reovirus. Avian Dis. 44**,** 638–664

Varela. R., Martinez-Costas, J., Mallo, M., Benavente, J., 1996. Intracellular posttranslational modifications of S1133 avian reovirus proteins. J. Virol. 70, 2974–2981.

Yuan, J., Adamski, R., Chen, J., 2010. Focus on histone variant H2AX: To be or not to be. FEBS Lett. 584, 3717–3724.

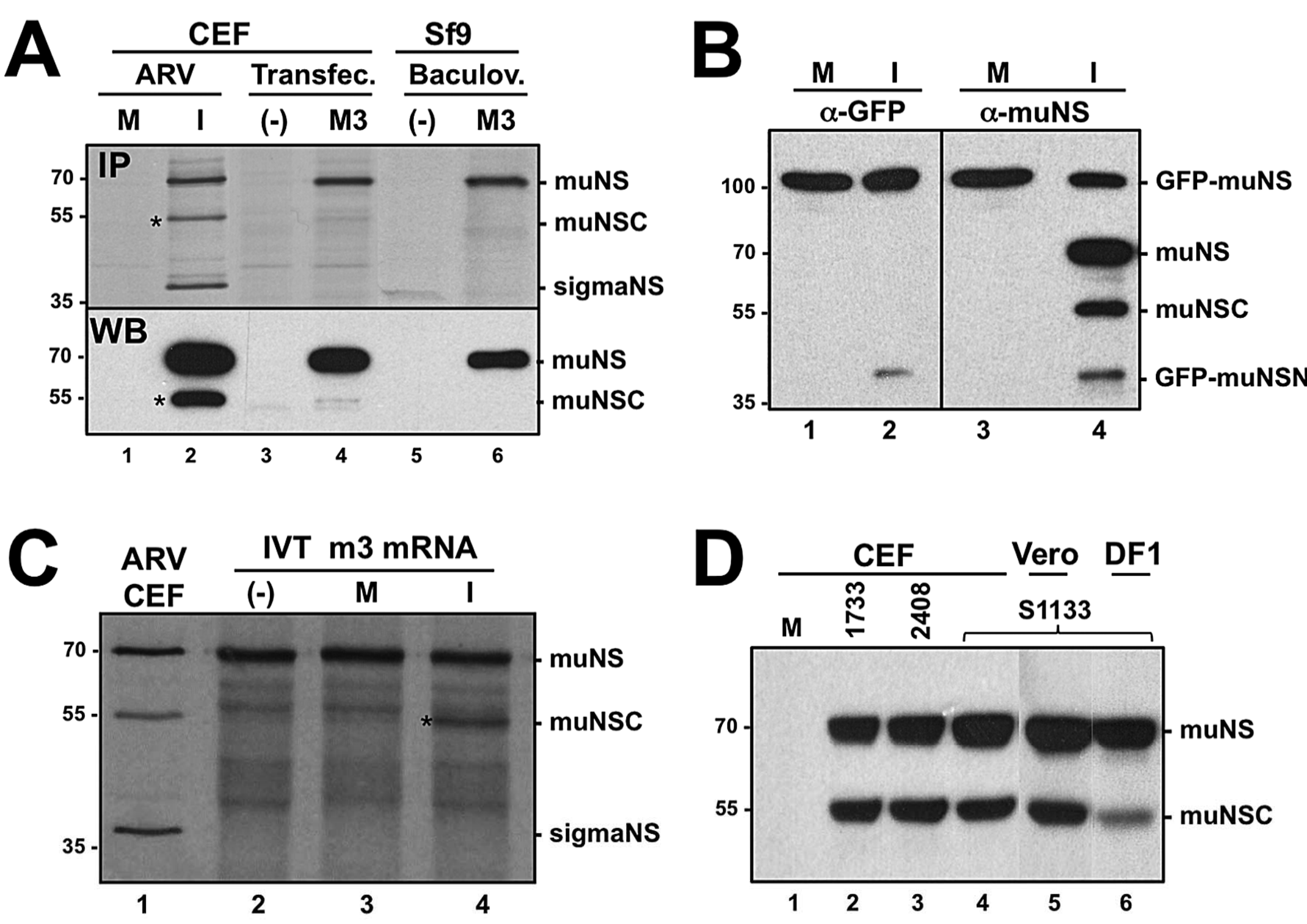
A
CEF
Sf9
ARV
Transfec.
Baculov.
M
I
(-)
M3
(-)
M3
IP
WB
70
55
35
*
muNS
muNSC
sigmaNS
1
2
3
4
5
6
B
M
I
M
I
α-GFP
α-muNS
100
70
55
35
GFP-muNS
muNS
muNSC
GFP-muNSN
1
2
3
4
C
ARV
CEF
IVT m3 mRNA
(-)
M
I
70
55
35
*
muNS
muNSC
sigmaNS
1
2
3
4
D
CEF
Vero
DF1
M
1733
2408
S1133
70
55
muNS
muNSC
1
2
3
4
5
6

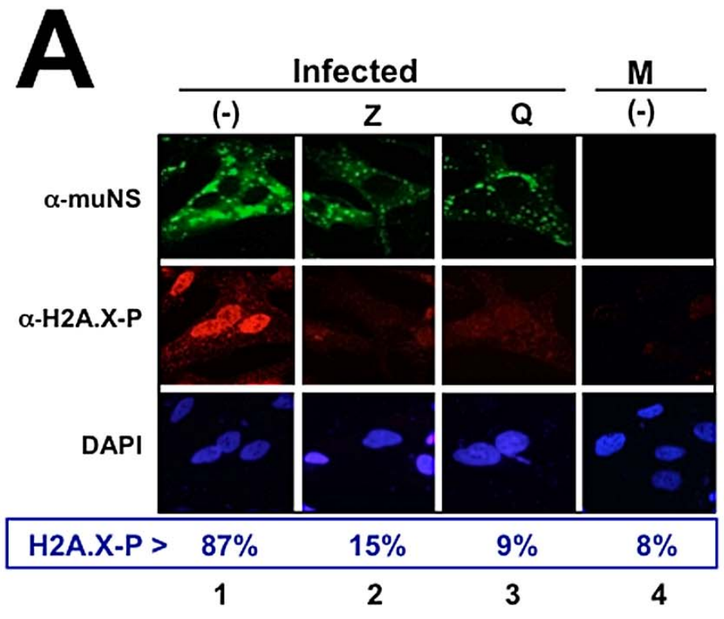
A
Infected
M
(-)
Z
Q
(-)
α-muNS
α-H2A.X-P
DAPI
H2A.X-P > 87% 15% 9% 8%
1 2 3 4

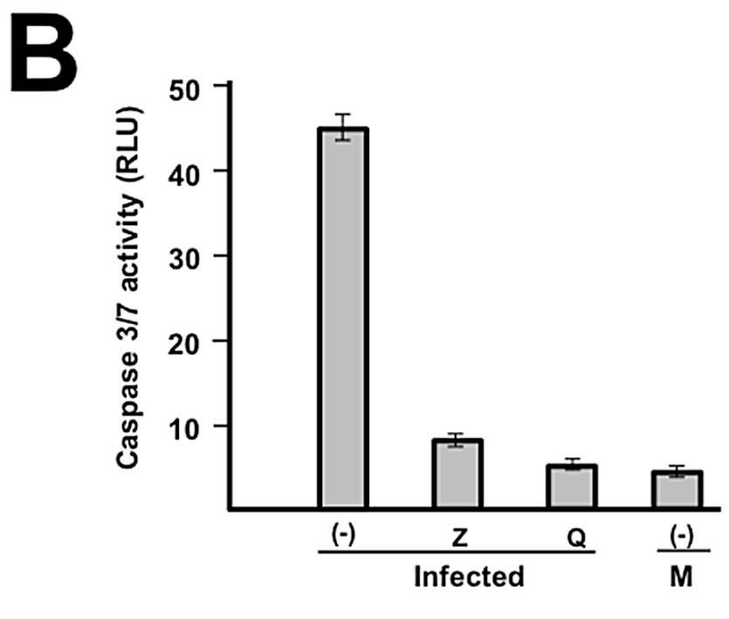
B
Caspase 3/7 activity (RLU)
50
40
30
20
10
(-)
Z
Q
(-)
Infected
M

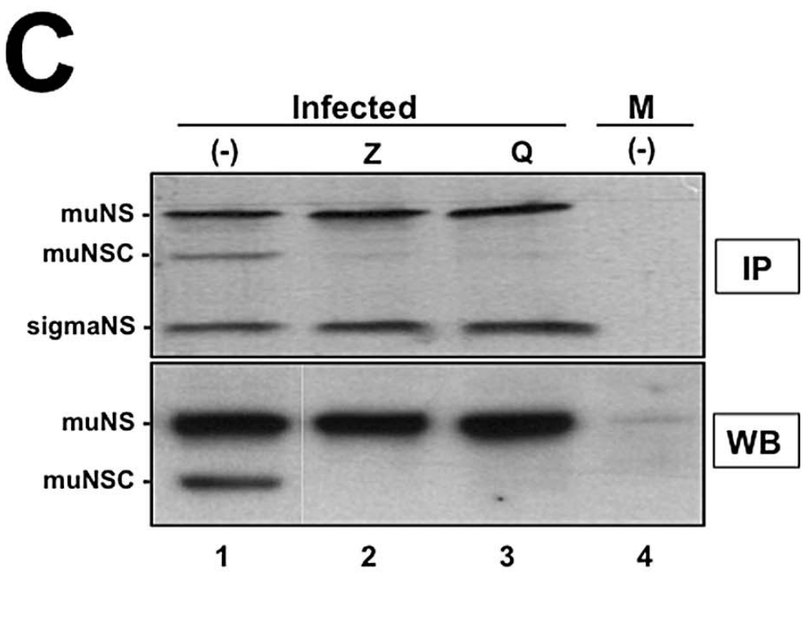
C
Infected
M
(-)
Z
Q
(-)
muNS
muNSC
sigmaNS
IP
muNS
muNSC
WB
1 2 3 4

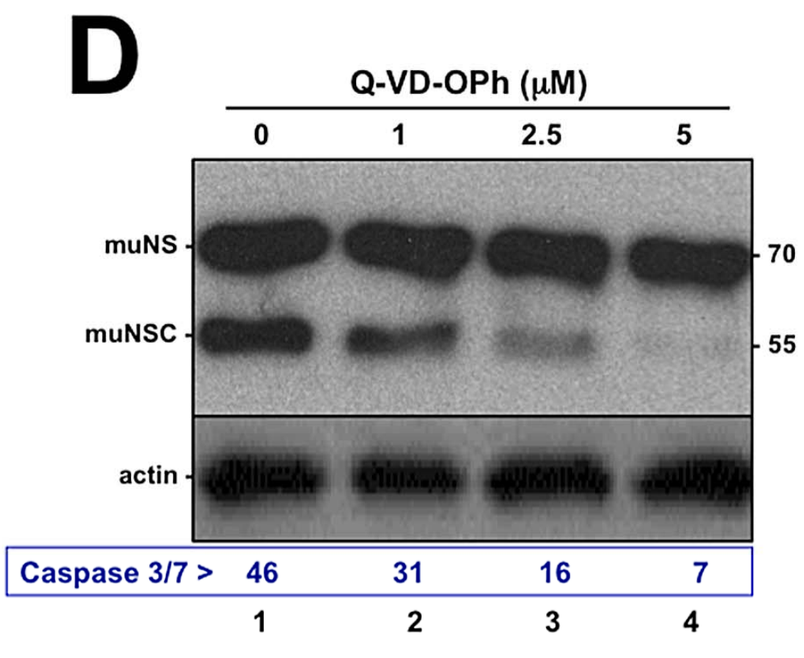
D
Q-VD-OPh (μM)
0 1 2.5 5
muNS
muNSC
70
55
actin
Caspase 3/7 > 46 31 16 7
1 2 3 4

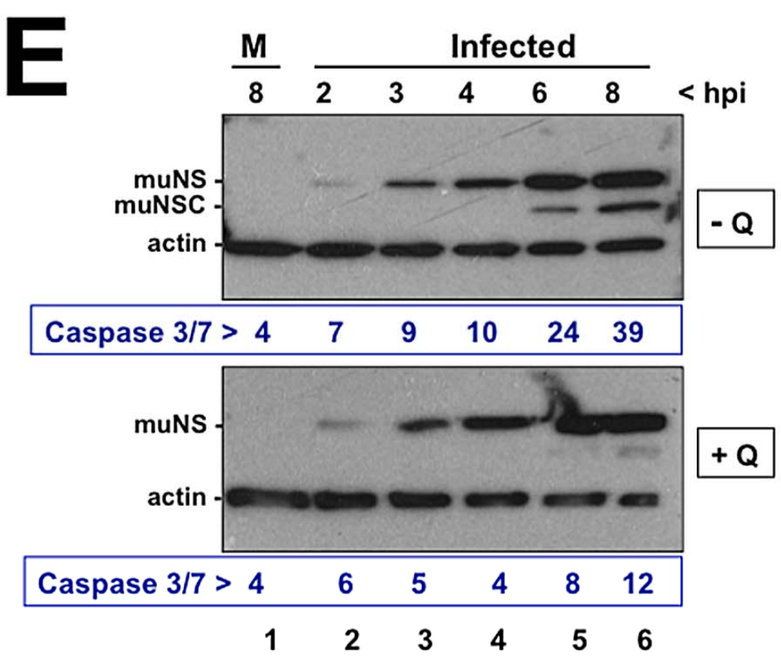
E
M
Infected
8 2 3 4 6 8 < hpi
muNS
muNSC
actin
- Q
Caspase 3/7 > 4 7 9 10 24 39
muNS
actin
+ Q
Caspase 3/7 > 4 6 5 4 8 12
1 2 3 4 5 6

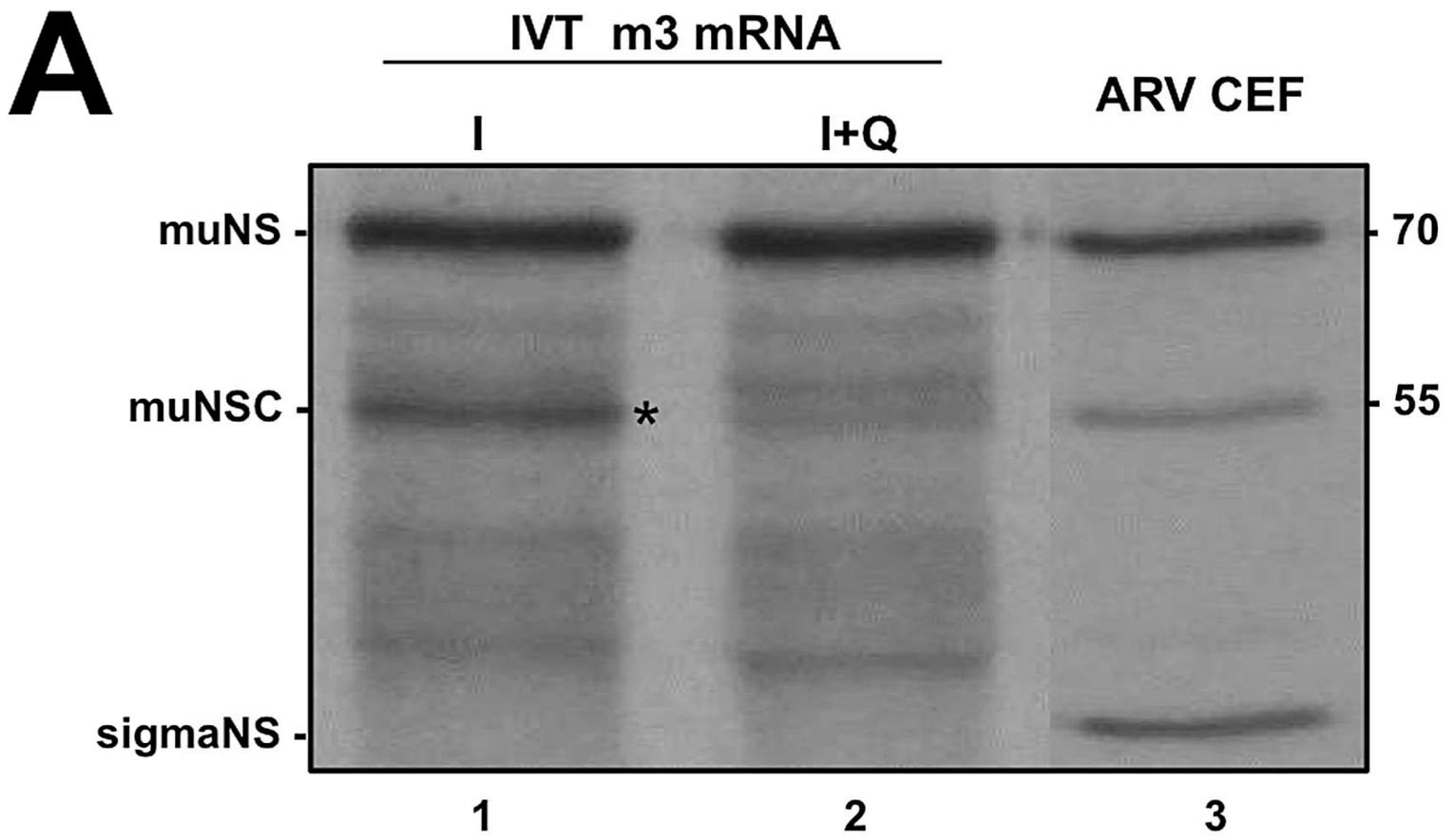

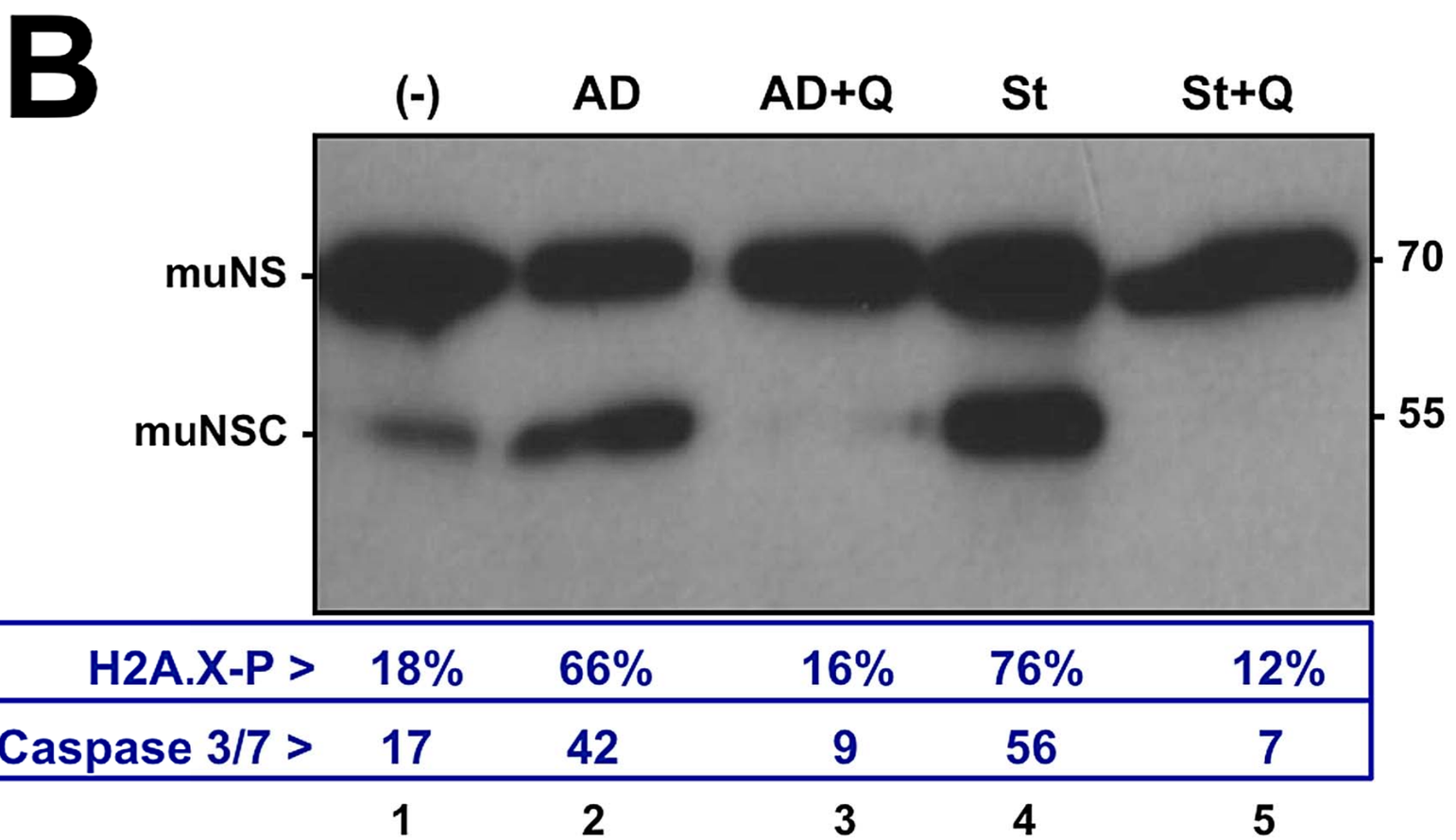

H2A.X-P >	18%	66%	16%	76%	12%
Caspase 3/7 >	17	42	9	56	7
	1	2	3	4	5

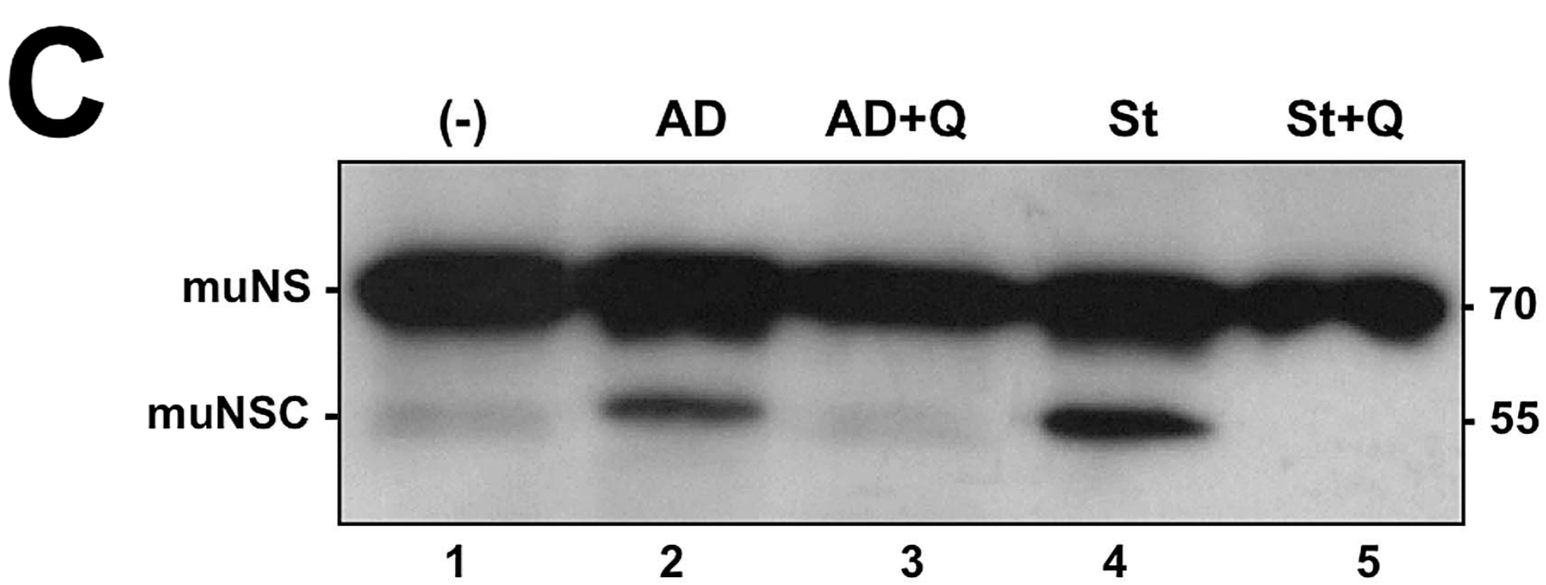

A

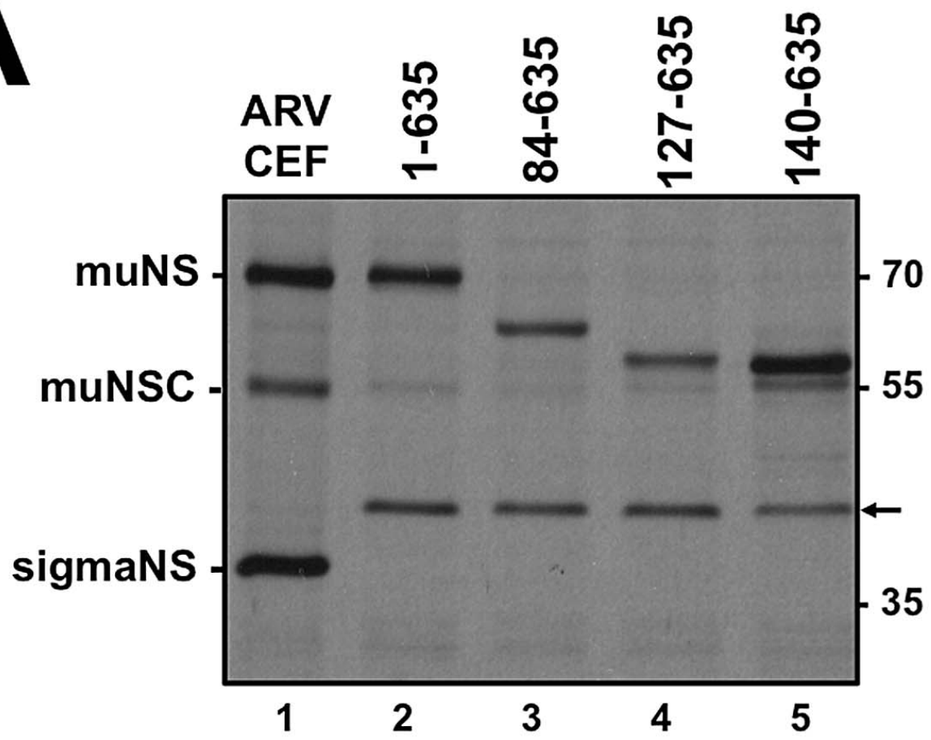

B

^{140}MVGTLEAVSTADSPDACAPVTSKILAKQQTIAKSPGRL^{177}

C

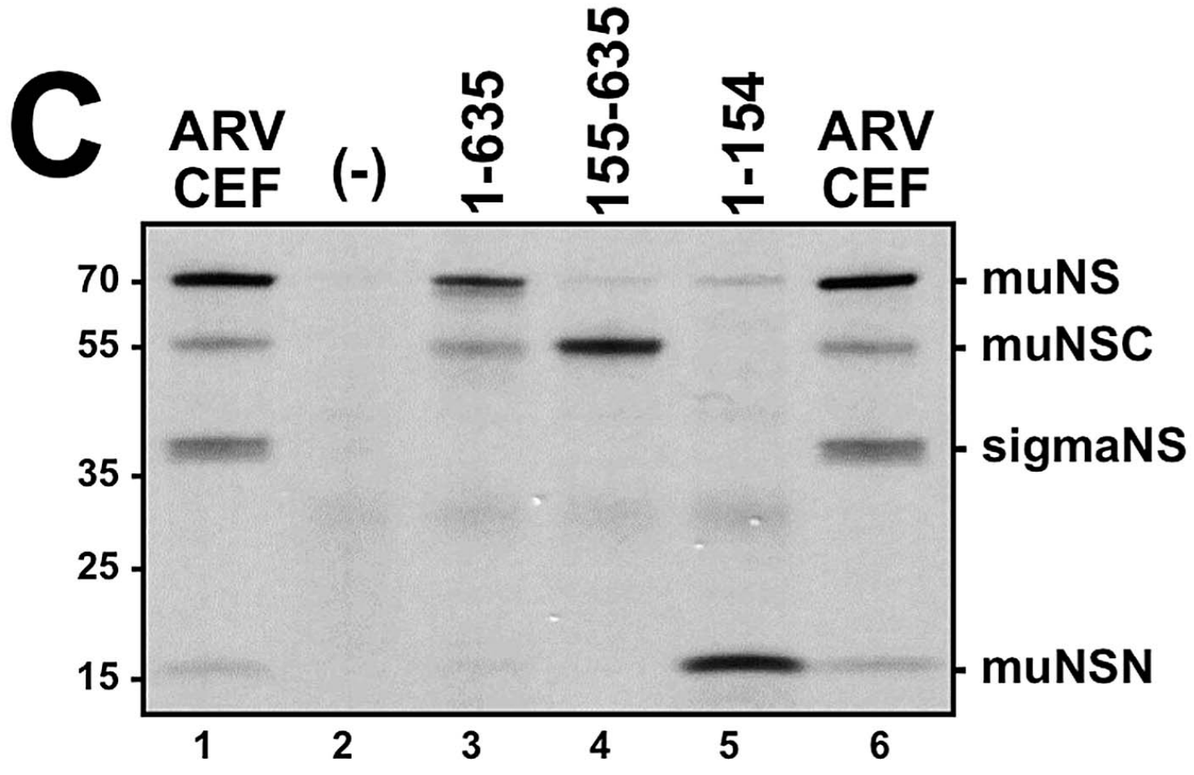

D

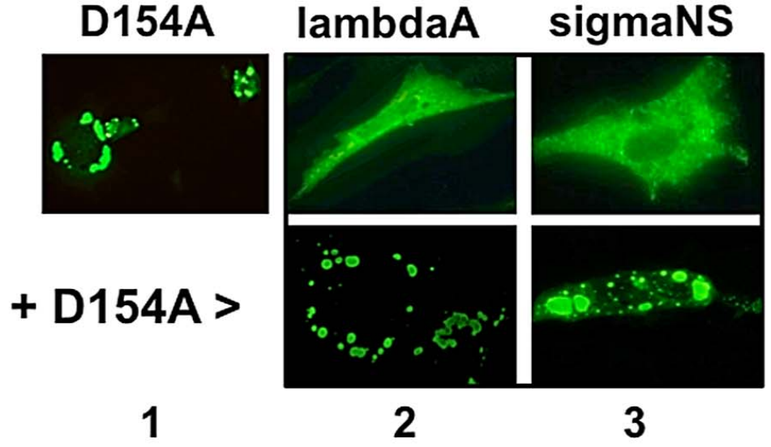

E

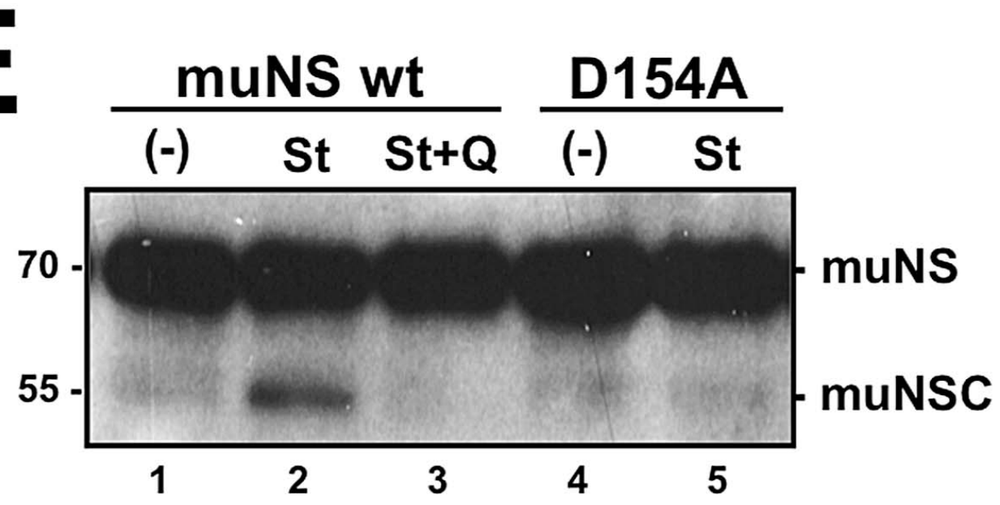

F

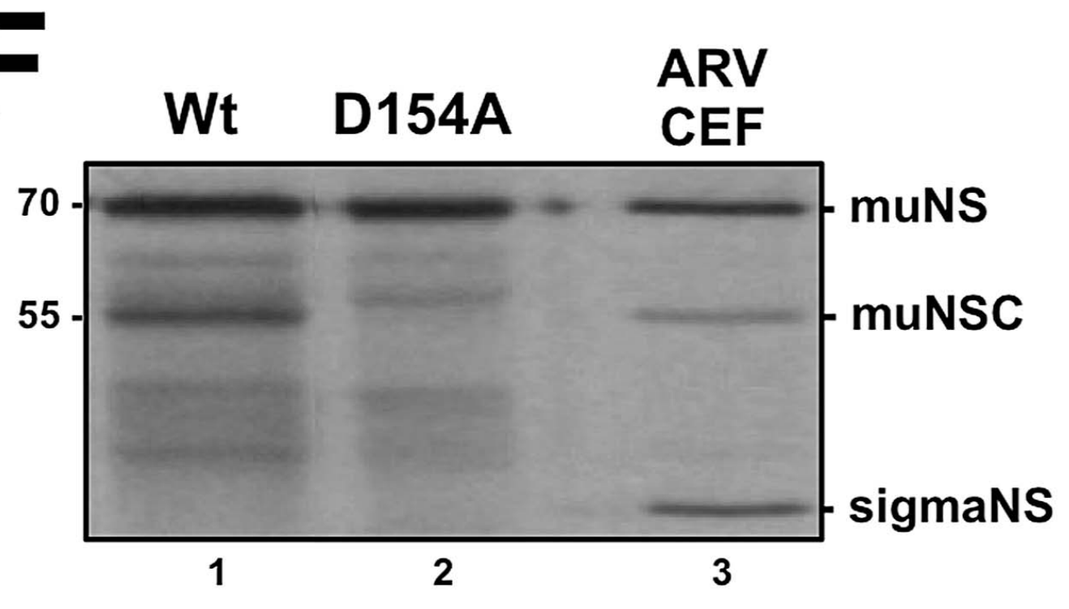

A

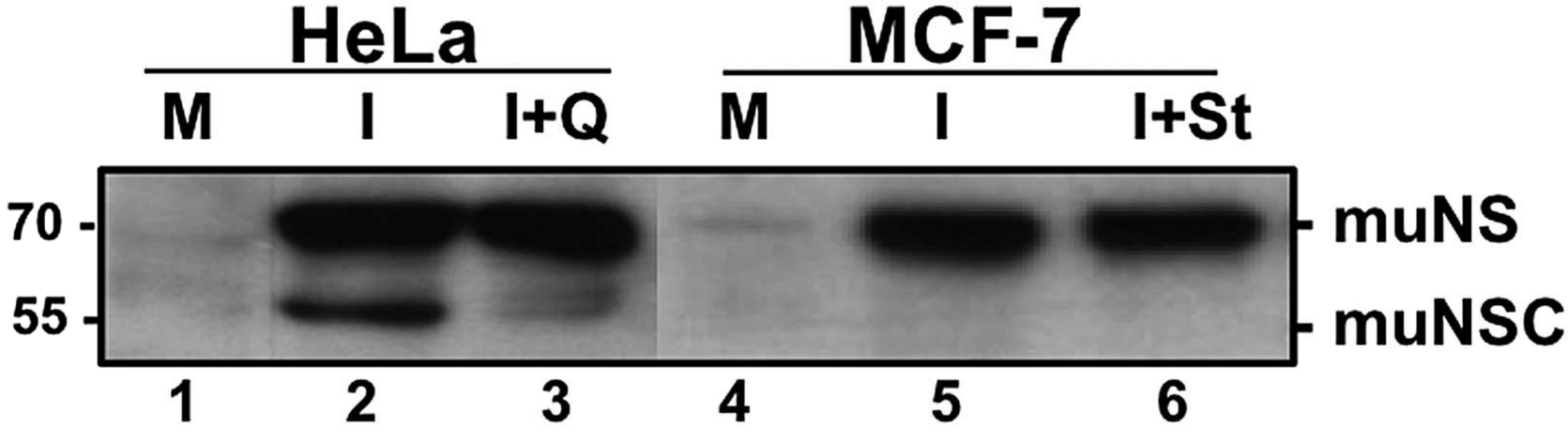
HeLa
MCF-7
M
I
I+Q
M
I
I+St
70
55
muNS
muNSC
1
2
3
4
5
6

B

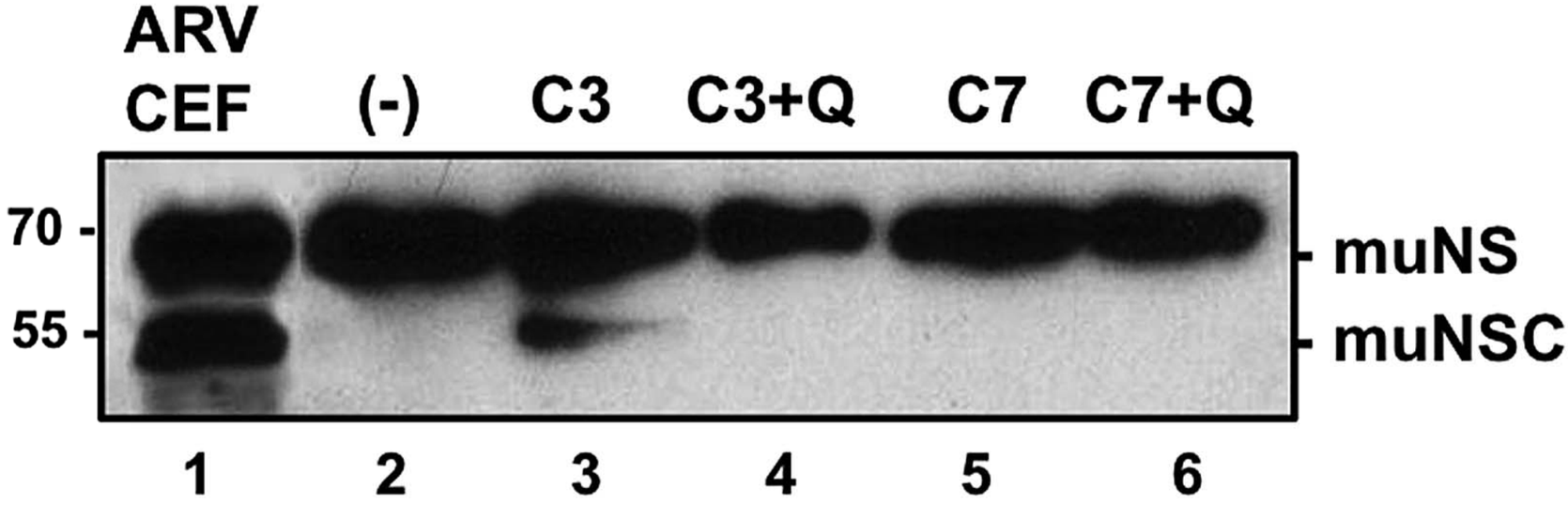
ARV
CEF
(-)
C3
C3+Q
C7
C7+Q
70
55
muNS
muNSC
1
2
3
4
5
6

A

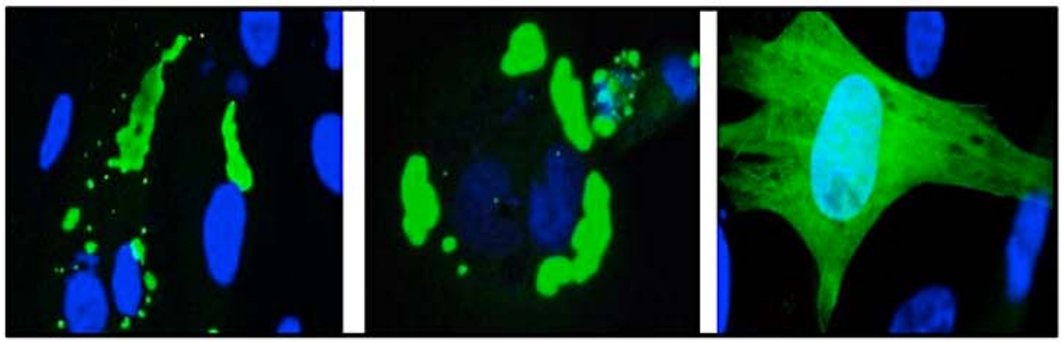
1-635
155-635
1-154

C

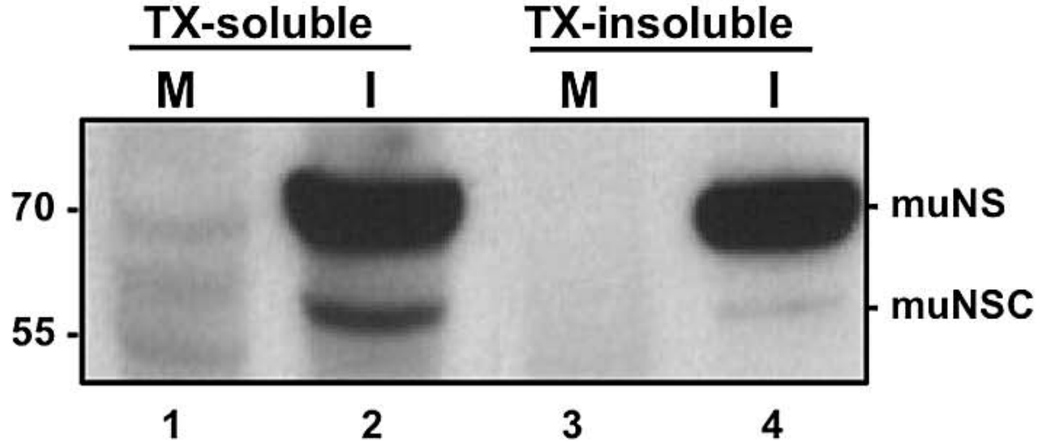
TX-soluble
TX-insoluble
M
I
M
I
70
55
muNS
muNSC
1
2
3
4

B

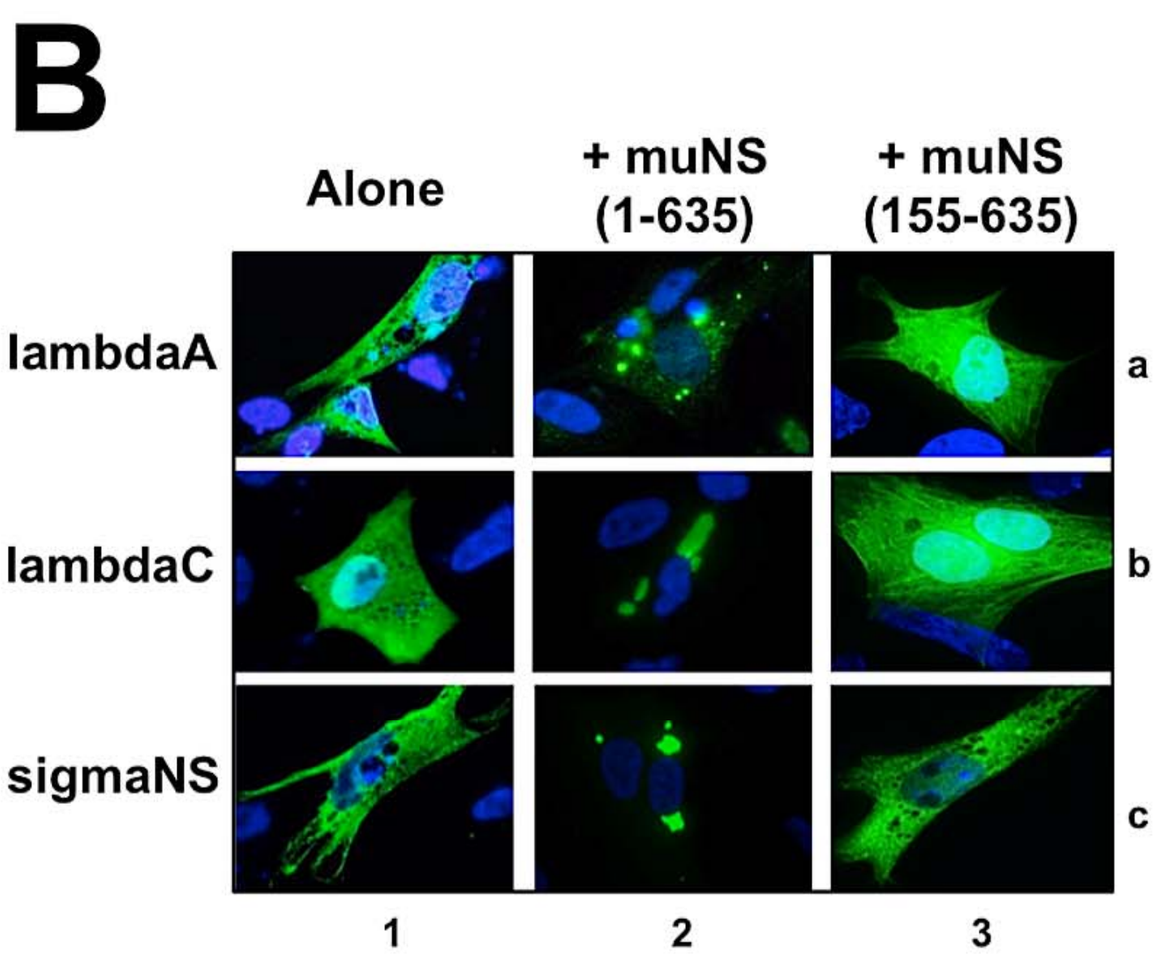
Alone
+ muNS (1-635)
+ muNS (155-635)
lambdaA
lambdaC
sigmaNS
a
b
c
1
2
3

D

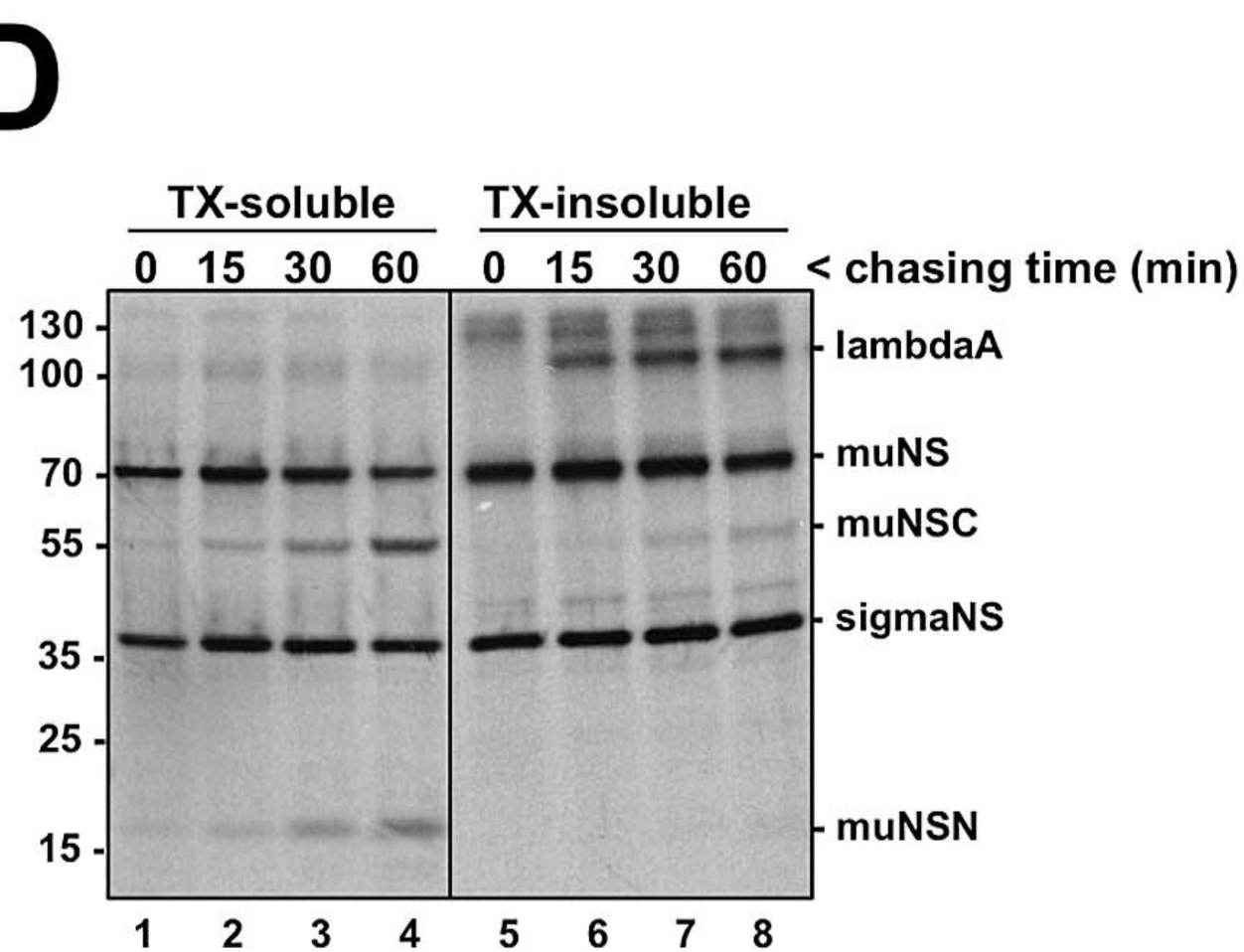
TX-soluble
TX-insoluble
0 15 30 60
0 15 30 60
< chasing time (min)
130
100
70
55
35
25
15
lambdaA
muNS
muNSC
sigmaNS
muNSN
1 2 3 4 5 6 7 8

A

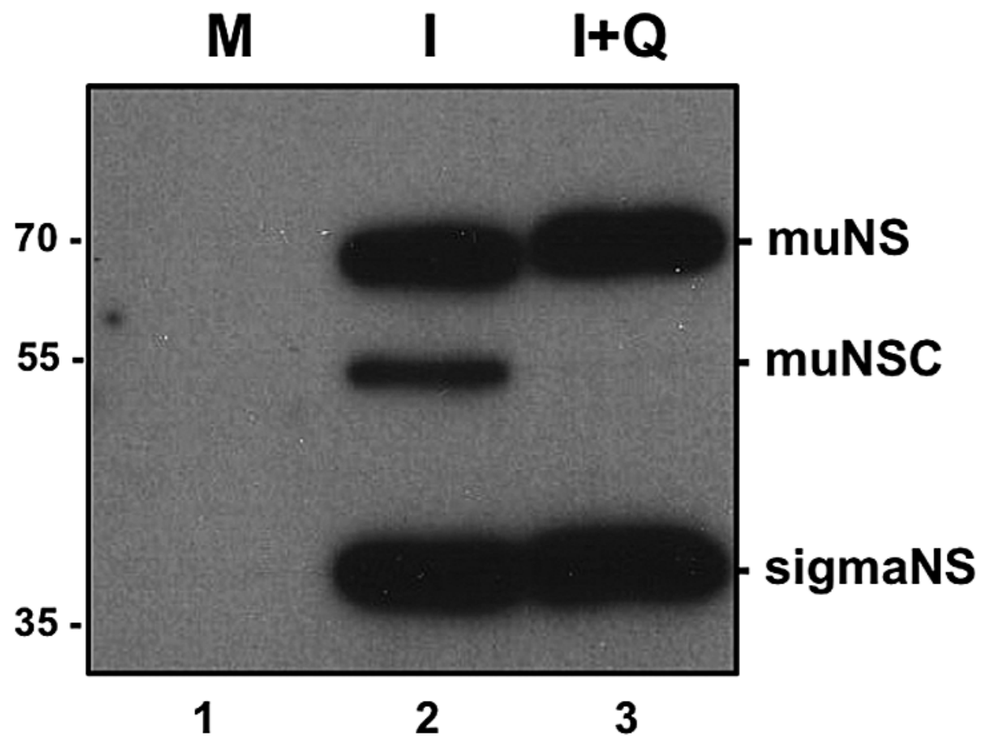
M
I
I+Q
70
55
35
muNS
muNSC
sigmaNS
1
2
3

B

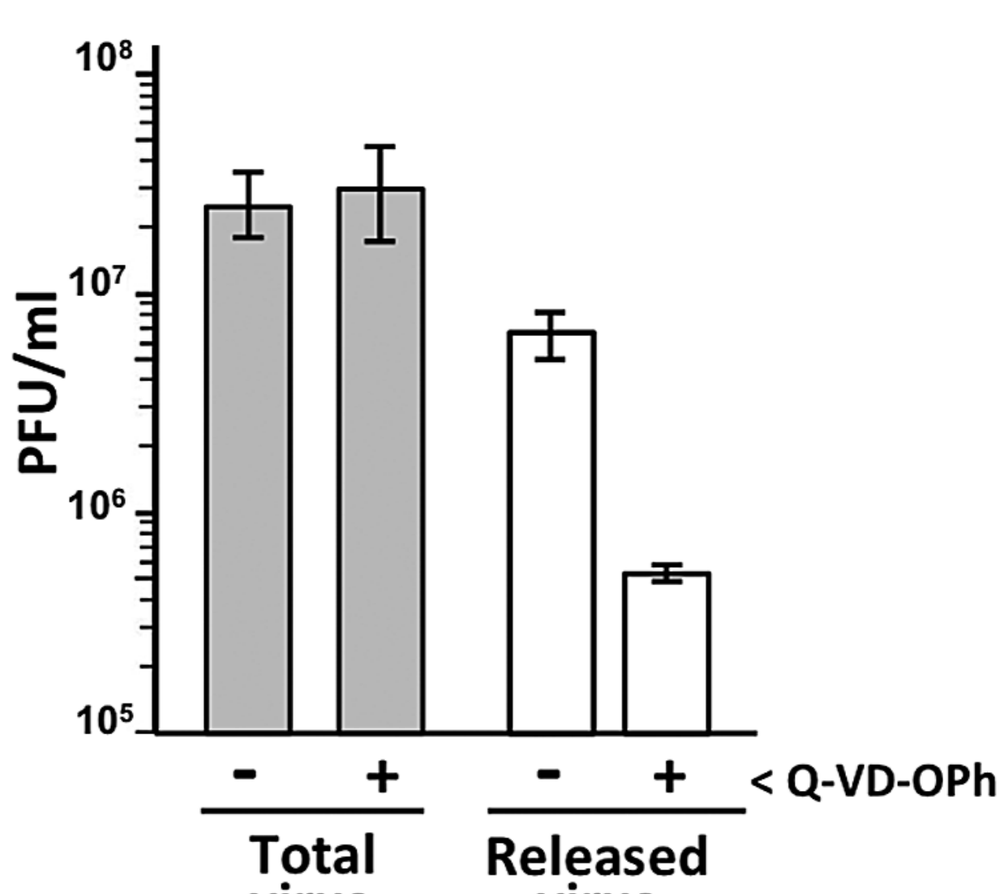
PFU/ml
10^8
10^7
10^6
10^5
-
+
-
+
< Q-VD-OPh
Total virus
Released virus

C

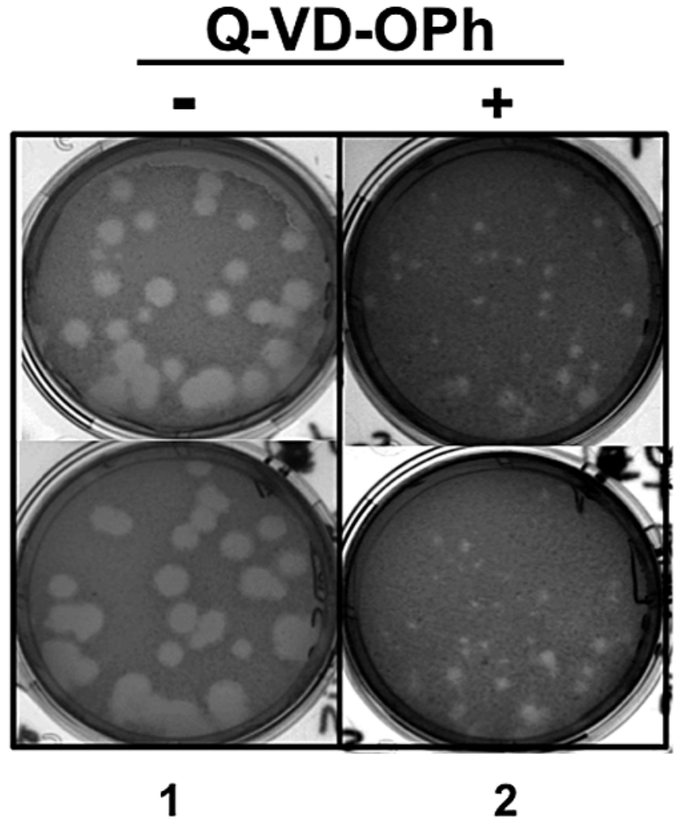
Q-VD-OPh
-
+
1
2

Source	Strain	Amino acid sequence of muNS region 140-177			Accession #
Chicken	S1133	140	MVGTLEAVSTADSPDACVPVTSKILAKQQTIAKSPGRL	177	AAS78987
	1733	140	MVGTLEAVSTADSPDACVPVTSKILAKQQTIAKSPGRL	177	AAQ81873.1
	2408	140	MVGTLEAVSTADSPDACVPVTSKILAKQQTIAKSPGRL	177	AAS78990.1
	176	140	MVGTLEAVSTADSPDACVPVTSKILAKQQTIAKSPGRL	177	AAT52027.1
	T-98	140	MVGTLEAVSTADSPDACVPVTSKILAKQQTIAKSPGRL	177	ACC77964.1
	C-98	140	MVGTLEAVSTADSPDACVLVTSKILAKQQTIAKSPGRL	177	ACC77965.1
	T-6	140	MVGTLEAVSTADSPDACVPVTSKILAKQQTIAKSPGRL	177	AAS78998.1
	GuangxiR1	140	MVGTLEAVSTADSPDACVPVTSKILAKQQTIAKSPGRL	177	AGM48324.1
	138	140	MVGALEAVSTVHSPDACVPDTAKILAKQQTIAKSPGRL	177	AAT52026.1
	750505	140	MVGTLEAVSTAHSPDACVPVPSKIIAKQQTIAKSPGRL	177	AAS78992.1
	916SI	140	MVGTLEAVSTAHSPDACVPVPSKIIAKQQTIAKSPGRL	177	AAS78993.1
	601G	140	MVGTLEAVSTAHSPDACVPVPSKIIAKQQTIAKSPGRL	177	AAS78991
	AVS-B	140	MVGTLEAVSTAHEPDACVPVTSKVVTKQQTIAKSPGRL	177	CBX25028.1
	918	140	MAGTLDAVSAVHEPDACVPVTSKIIAKQQTASKSPGRL	177	AAS78994.1
	1017-1	140	MAGTLDAVSAVHEPDACVPVTSKIIAKQQTASKSPGRL	177	AAS78988.1
	R2	140	MAGTLDAVSAVHEPDACVPVTSKIIAKQQTASKSPGRL	177	AAS78997.1
	T1781	140	MAGTLDAVSAVHEPDACVPVTSKIVAKQQTMSKSPGRL	177	AGO32036
Quail →	919	140	MVGTLEAVSTADSPDACVPVTSKILAKQQTIAKSPGRL	177	AAS78995.1
Duck	091	140	MAGTMDAVSTGHPPGASVPDVSKVVAKQQTISKSPGRL	177	AFV52262.1
	TH11	140	MAGTMDAVSTGHPPGASVPDVSKVVAKQQTISKSPGRL	177	AFU11110.1
	NP03	140	MAGTMDAVSTGHPPGASVPDVSKVIAKQQTISKSPGRL	177	AEA92265
	ZJ00M	140	MAGTMDAVSTGHPPGASVPDVSKVVAKQQTISKSPGRL	177	AHF47511
	J18	140	MAGTMDAVSTGHPPGASVPDVSKVVAKQQTISKSPGRL	177	CAC82380.1
	89330	140	MAGTMDAVSTGHPPGASVPDVSKVVAKQQTISKSPGRL	177	AFV52274.1
	ZJ2000M	140	MAGTMDAVSTGHLPGASVPDVSKMVAKQQTISKSPGRL	177	AGY49083
	S14	140	MAGTMDAVSTGHLPGASVPDVSKVVAKQQTISKSPGRL	177	ABJ80883.1
	815-12	140	MAGTMDAVSTGHLPGASVPDVSKVVAKQQTISKSPGRL	177	AGO58397.1
	MW9710	140	MAGTMDAVSTGHLPGASVPDVSKVVAKQQTISKSPGRL	177	EF581012.1
Goose →	03G	140	MAGTMDAVSTGHPPGASVPDVSKVVAKQQTISKSPGRL	177	AFQ62083.1